



## Development of Risk Informed In-Service Inspection Analysis Procedures and Application to Finnish BWR Unit Piping Components

Authors: Otso Cronvall, Ilkka Männistö and Jouni Alhainen




Confidentiality: Public

Report's title Development of Risk Informed In-Service Inspection Analysis Procedures and Application to Finnish BWR Unit Piping Components	
Customer, contact person, address State Nuclear Waste Management Fund (VYR), Nordic Nuclear Safety Research (NKS) and Technical Research Centre of Finland (VTT)	Order reference
Project name PURISTA	Project number/Short name 13109
Author(s) Otso Cronvall, Ilkka Männistö and Jouni Alhainen	Pages 48/0
Keywords RI-ISI, risk matrix, EPRI procedure, SCC, FAC, PFM, Markov system, pipe rupture probability, inspection program, POD	Report identification code VTT-R-00650-09
<p>Summary</p> <p>The main emphasis of this study is on the recent developments in the probabilistic fracture mechanics (PFM) based analysis code VTTBESIT as well as on widening the analysis scope through application of an existing PFM procedure not applied before in Finland, at least to the author's knowledge. Assessment of probabilistic distributions for depth and length of initial cracks induced by stress corrosion cracking (SCC) was added to the analysis scope. The new analysis developments and extensions were applied a Finnish Boiling Water Reactor (BWR) plant. The results from these simulations are used as input data for calculating piping leak/break probabilities using a Markov system approach. Piping leak/break probabilities are combined with evaluations of consequences of piping failures to obtain the risk importance of piping in the risk informed in-service inspection (RI-ISI) analyses.</p> <p>The developed approach to assess the probabilistic distributions of the sizes of initial cracks induced by SCC from the data of detected cracks is summarized here. So, the recursive assessment approach applied here is such that first the size data concerning detected grown SCC induced cracks, as obtained through screening from the used crack database, is converted to dimensionless form in relation to pipe wall thickness and inner circumference. Then, with fracture mechanics based analyses, the thus obtained data is matched with the assumed initial sizes, the criterion for which here is to correspond to respective mode I stress intensity factor threshold values, <math>K_{I,threshold}</math>, for SCC initiated cracks. Finally, the thus obtained data is converted to probabilistic form and a suitable reliability distribution function is fitted to it.</p> <p>The modelling approaches were applied to selected piping segments of the Shut-down cooling system 321 and Reheater and moisture separator system 412 of Nuclear Power Plant (NPP) unit OL1 of TVO. The analysed degradation mechanisms were SCC and flow accelerated corrosion (FAC) The loads considered in the analyses were pressure and temperature under stationary operational conditions, as well as stationary welding process induced residual stresses in the welds. The analysed crack postulates were assumed to be located in the inner surface of the piping welds in case of SCC. In case FAC local wall thinning due to corrosion and starting from the inner surface was analysed. The quantitative probabilistic results from these PFM analyses can be used further in the consequent RI-ISI analyses.</p> <p>In this study the purpose is also to compare the effect of the two sets of probabilistic distributions for initial sizes of SCC induced cracks during operation to the pipe rupture probabilities. This was carried out by comparing the new PFM results obtained here for a selection of piping welds from the OL1 system 321 to the corresponding earlier results for the same welds presented in ref. [7]. The probabilistic initial crack sizes are according to the new distributions developed in this study considerably smaller than those according to the earlier study, see ref. [7]. For instance for the former distributions the mean crack depth is approximately 300 <math>\mu\text{m}</math>, whereas for the latter ones approximately 1000 <math>\mu\text{m}</math>, respectively. This is consequently reflected in the yearly pipe rupture probability results obtained from the Markov application analyses, as with the former distributions it is for most of the duration of the assumed 60 years of operational plant lifetime approximately 100 times smaller than</p>	

with the latter ones. This is a quite large difference, and indicates that the selection of the probabilistic distributions for initial sizes of SCC induced cracks during operation has a great impact on the consequent yearly pipe rupture probability results, an aspect which is useful to keep in mind e.g. when attempting to avoid unnecessary conservatism in the PFM and RI-ISI analyses. Concerning all cases and both input data sets, the yearly pipe rupture probability results vary approximately between  $10E-10$  to  $10E-4$ .

It is considered that improved PFM based analysis scope and accuracy provide valuable support to overall quantitative assessment of piping weld failure potentials. In general, the favoured option for quantitative piping failure potential assessment would be statistical analysis of piping degradation data. However, there most often does not exist enough applicable degradation data for this, and thus structural reliability methods, most relevant for this purpose being PFM, need to be resorted to. So, having both cracking data and PFM analysis results gives a much better and in scope wider information basis for experts to plant specifically assess the piping weld failure potentials, and consequently leads to more accurate and detailed RI-ISI analysis results. As with other RI-ISI related analysis procedures, also PFM has its uncertainties and accuracy challenges; however PFM analyses on the other hand easily allow making extensive sensitivity analyses for the involved physical analysis input parameters. It should be mentioned, though, that PFM analyses alone do not yet suffice to be the sole basis for piping failure potential quantification.

The accuracy of the analysis procedures covered here is considered to be at least reasonable, and mostly or arguably in all cases to some extent conservative. Thus the results obtained with these PFM procedures are considered to be useful for quantitative RI-ISI analysis purposes, also due to providing the above mentioned new developments. However, more important than the absolute result values are their comparison to each other, since based on that the failure potential classes in the RI-ISI risk matrix failure potential category can be defined.

Confidentiality	Public	
Espoo 20.3.2009		
Signatures	Signatures	Signatures
		
Accepted by Eila Lehmus Technology Manager	Written by Otso Cronvall Research Scientist	Checked by Kaisa Simola Senior Research Scientist
VTT's contact address P.O. Box 1000, 02044 VTT		
Distribution (customer and VTT) STUK: Registry (4), Vilpas M. (1 kpl); TVO: Hukkanen K. (1 kpl); VTT: Archive (2)		
<i>The use of the name of the VTT Technical Research Centre of Finland (VTT) in advertising or publication in part of this report is only permissible with written authorisation from the VTT Technical Research Centre of Finland.</i>		

## Preface

This report has been prepared under the research project PURISTA, which concerns Risk Informed In-service Inspection (RI-ISI) analyses of Nuclear Power Plant (NPP) piping systems. The project is a part of SAFIR2010, which is a national nuclear energy research program. PURISTA project work in 2008 was funded by the State Nuclear Waste Management Fund (VYR), the Nordic Nuclear Safety Research (NKS) and the Technical Research Centre of Finland (VTT). The work was carried out at VTT. The authors of the report express their gratitude to Mr Petri Kuusinen and Mrs Anneli Reinvall, both from TVO, for their valuable co-operation.

Espoo 20.3.2009

Authors

## Contents

Preface .....	3
1 Introduction.....	7
2 RI-ISI analysis methodology .....	9
2.1 Overview.....	9
2.2 New developments/applications in PFM modelling .....	10
2.2.1 The assessment of probabilistic distributions for sizes of initial cracks induced by SCC.....	11
2.2.2 Probabilistic FAC model.....	15
3 Comparative pipe leak/rupture probability analyses of the OL1 piping system 32120	
3.1 Overview of the piping system and its division to segments .....	20
3.2 Prevailing degradation mechanisms and selection of the analysed piping welds.....	20
3.3 Input data for PFM analyses .....	22
3.4 Crack growth simulations .....	24
3.4.1 Analysed cases.....	25
3.4.2 Analysis approach and crack growth equations .....	25
3.4.3 Analysis code VTTBESIT.....	27
3.4.4 Results from VTTBESIT analyses.....	28
3.5 Pipe component leak/rupture probability analyses.....	29
3.5.1 Analysis approach.....	29
3.5.2 Results from the Markov application analyses.....	31
4 Pipe leak/rupture probability analyses of the OL1 piping system 412.....	36
4.1 Short overview of the piping system .....	36
4.2 Input data for FAC analyses.....	36
4.3 Results from the probabilistic FAC analyses.....	37
5 Summary and conclusions.....	41
References .....	45

## List of symbols and abbreviations

### Latin symbols

$a$	Crack depth
$c$	Half of crack length
$a_i$	Depth of initiating crack
$B, N$	Flow Accelerated Corrosion model parameters
$C_1, C_2, C_3, C_4$	Flow Accelerated Corrosion model parameters
$C$	Consequence
$C_i$	Consequence of event $i$
$C_{SCC}$	Parameter in the stress corrosion cracking equation
$D$	Outer pipe diameter
$E$	Multiplicative adjustment factor
$f(t)$	Time correction factor
$F$	Flow rate
$g$	Oxygen content
$h$	Content of chromium and molybdenum in steel
$J_{Ic}$	Mode I $J$ -integral fracture toughness
$k_c$	Geometrical factor
$K_I$	Mode I stress intensity factor
$K_{I,threshold}$	Mode I stress intensity factor threshold
$K_{Ic}$	Mode I stress intensity fracture toughness against brittle fracture
$l_i$	Length of initiating crack
$\dot{m}$	Mass flux
$M_{deg}$	Degradation matrix
$M_{ins}$	Inspection matrix
$n_{SCC}$	Exponent in the stress corrosion cracking equation
$p$	Pressure
$P$	Probability
$pH$	fluid pH value
$P_i$	Probability of event $i$
$R$	Risk
$R_i$	Risk of event $i$
$R_i$	Inner pipe radius
$t$	Plant operation period
$t$	Time, exposure time
$t_{wall}$	Pipe wall thickness
$T$	Temperature
$w$	Flow velocity
$W_C(t)$	Thickness of the pipe wall corroded away
$W_{C,calculated}(t)$	Calculated thickness of pipe corroded away at time $t$
$W_F$	Mean velocity in the film of water on the wall of the component,
$W_{original}$	Original, nominal pipe wall thickness
$W_{pipe}(t)$	Pipe wall thickness at time $t$
$x$	Radial coordinate through pipe wall thickness having origin at inner surface
$x_{st}$	Steam quality

## Greek symbols

$\alpha$	Void fraction
$\Delta\phi_R$	Flow Accelerated Corrosion rate
$\Delta\phi_{R,KWU-KR}$	Specific deterministic Flow Accelerated Corrosion rate as predicted by the KWU-KR model
$\mu_E$	Scale parameter
$\sigma_a$	Axial membrane stress
$\sigma_{a,resid}$	Axial weld centre line residual stress
$\sigma_E$	Shape parameter
$\rho_{st}$	Density of steel
$\rho_w$	Density of the water at saturation condition

## Abbreviations

ASME	American Society of Mechanical Engineers
BWR	Boiling Water Reactor
CCDF	Conditional Core Damage Frequency
CCDP	Conditional Core Damage Probability
CLRP	Conditional Large Release Probability
CLERP	Conditional Large Early Release Probability
EPRI	Electric Power Research Institute
FAC	Flow Accelerated Corrosion
FEM	Finite Element Method
HAZ	Heat affected zone
ISI	In-Service Inspection
IWM	Fraunhofer-Institut für Werkstoffmechanik
LHS	Latin Hypercube Sampling
LOCA	Loss Of Coolant Accident
LWR	Light Water Reactor
NKS	Nordic Nuclear Safety Research
NPP	Nuclear Power Plant
OL1	Olkiluoto 1 Nuclear Power Plant
OL2	Olkiluoto 2 Nuclear Power Plant
PFM	Probabilistic Fracture Mechanics
POD	Probability Of Detection
PSA	Probabilistic Safety Assessment
RPV	Reactor Pressure Vessel
RI-ISI	Risk Informed In-Service Inspection
SCC	Stress Corrosion Cracking
SIF	Stress Intensity Factor
SMAW	Shielded Metal Arc Welding
STUK	Radiation and Nuclear Safety Authority (SäteilyturvaKeskus)
TVO	Teollisuuden Voima Oyj
VTT	Technical Research Centre of Finland
VYR	State Nuclear Waste Management Fund

## 1 Introduction

The aim of this study is to continue the development of probabilistic fracture mechanics (PFM) analysis approaches to quantify piping failure probabilities. Quantitative measures of piping failures are used e.g. in quantitative risk-informed in-service inspection (RI-ISI) applications. As there often does not exist enough applicable degradation data of piping systems to allow the use of statistical methods in quantifying the failure potential, structural reliability methods are a way to overcome this problem.

Probabilistic version of fracture mechanics based analysis code VTTBESIT was used to simulate the crack growth through wall in a selection of weld cross-sections of the Shut-down cooling system (321) piping of TVO nuclear power plant (NPP) unit OL1. The probabilistic capabilities of the code were developed further in the project. The analyses with a further developed PFM procedure presented here compare to earlier PFM and RI-ISI analyses performed to the same piping system, and also by the same authors, see ref. [7].

For the system 321 the analysed degradation mechanism was stress corrosion cracking (SCC), which according to ref. [2] is one of the prevailing degradation mechanisms this piping system is susceptible to. The loads considered in the analyses were pressure and temperature under stationary operational conditions, as well as stationary welding process induced residual stresses in the welds. The analysed crack postulates were assumed to be located in the inner surface of the piping welds.

The piping leak and break probabilities were calculated with a Markov process application developed earlier, see ref. [7], and realised with Matlab code. This application includes also the effects of inspections, and thus the capability to analyse various inspection strategies.

PFM analyses were also performed to one piping component in the Reheater and moisture separator system 412. There the analysed degradation mechanism was Flow Accelerated Corrosion (FAC). It was assumed that the system 412 is among those few in Boiling Water Reactor (BWR) plants where FAC could potentially occur. The loads considered in these analyses were flow rate and fluid chemistry properties under stationary operational conditions. With the applied FAC model it was possible to assess the probabilistic wall thinning rate due to FAC starting from the inner surface of the piping component base material towards its outer surface.

The authors are grateful for Mr Petri Kuusinen and Mrs Anneli Reinvall from TVO for providing the needed technical input data concerning the analysed piping cases and for most pleasant co-operation.

Such quantitative probabilistic assessments of piping component failures as described above are needed as input data along with quantitative estimates of the failure consequences, as taken from the plant specific PSA, in the quantitative RI-ISI analyses for NPP piping systems.



In general the structural reliability analyses necessitate a thorough knowledge of structural properties, loads, the relevant ageing mechanisms and prevailing environmental conditions of the examined system/component.

The report summarises the VTT RI-ISI methodology framework, and focuses on highlighting the new features added and improvements developed to the PFM analysis capabilities. Further, applications to selected piping components of the OL1 piping systems 321 and 412 are presented.

## 2 RI-ISI analysis methodology

### 2.1 Overview

The purpose of RI-ISI analysis methodology is to allow the comparison of different in-service inspection (ISI) strategies for NPP piping, in respect to their effect on plant risk. The most common definition of risk is probability times the consequences:

$$R = P \cdot C \quad (2.1.1)$$

where  $R$  is the risk,  $P$  is the probability of the event studied and  $C$  is the amount of negative consequences caused by the event. The main focus of this study is in the calculation of the leak/rupture probability  $P$  for piping components with the above equation. The consequences of pipe leak/rupture are determined from the probabilistic safety assessment (PSA) as conditional core damage probability (CCDP) and conditional large early release probability (CLERP) values (or conditional large release probability (CLRP) values), and they have been determined for the analysed system in the previous studies, see refs. [4, 7].

To calculate the leak/rupture probability, two distinct parts of ISI are modelled: the phenomenon of crack growth and the activity of inspecting the pipes. These both affect the probability or frequency of pipe leaks/ruptures. In addition to this, PSA is used to evaluate the consequences of pipe rupture.

The goal of modelling crack growth is to calculate leak/rupture probability densities for a piping component, segment and/or system, depending also on the affecting degradation mechanisms in question. This information is combined in a Markov model where the different distinct states correspond to different depths of the crack growth process, for methodology background see e.g. refs. [5, 6]. A discrete time Markov procedure was chosen for easier applicability as compared to different inspection strategies by using two different Markov matrices. The overall method can be summarised in six steps:

- 1) Crack growth simulations based on PFM.
- 2) Construction of degradation matrix transition probabilities from PFM simulations and database analysis of crack initiation frequencies.
- 3) Model for inspection quality, which is used to construct inspection matrix transition probabilities.
- 4) Markov model to calculate pipe leak/rupture probabilities for chosen inspection schemes.
- 5) Assessment of pipe rupture consequences from PSA.
- 6) Comparison of results for different inspection strategies. Measures of interest include yearly rupture leak/probability, yearly core damage probability and average values for both of these over plant lifetime.

The RI-ISI risk classification method developed by VTT, as reported in ref. [4], is applied in step 6. It is a developed modification of the EPRI classification method

[1, 3], and includes quantified measures for both probabilities and consequences of the pipe leak and rupture.

## 2.2 New developments/applications in PFM modelling

The probabilistic treatment of some of the crack growth analysis input data parameters as well as application of probabilistic procedures are described in this section. The crack growth analyses concerning SCC were performed by applying a fracture mechanics based analysis tool VTTBESIT, the continuing development of which is provided by VTT. The wall thinning analyses concerning FAC were performed with spread sheet calculations. However, it is the aim to implement the probabilistic FAC model to the above mentioned fracture mechanics based analysis tool. Other crack growth and wall thinning analysis input data parameters than those presented here as probabilistically distributed were considered to have deterministic values.

In general, several of the input data parameters relevant in fracture mechanics and wall thinning analyses have markedly scattered characteristics, which can be observed e.g. from laboratory test results. Due to this a more realistic approach than to use single values for these parameters, as is done in deterministic analyses, is to consider such parameters as distributed, which is the approach followed in probabilistic analyses.

Fracture mechanics analysis input data parameters which have scattered characteristics include [8]:

- dimensions of existing manufacturing cracks; depth and length,
- dimensions of initiating cracks; depth and length,
- formation frequency of initial cracks,
- certain material properties; e.g. fracture toughness, tensile stress,
- service conditions; e.g. frequencies of load cycles.

In this study probabilistic distributions were developed for two input data parameters, which are:

- depth of initiating SCC cracks,
- length of initiating SCC cracks.

Also other input data parameters could have been considered as distributed, however due to lack of available input data this was not feasible. On the other hand, when more parameters are considered as distributed, the analyses become computationally considerably more laborious. However, it is often sufficient from the viewpoint of the quality of probabilistic analysis results to consider only some (at least two or three) of the most relevant scattered input data parameters as distributed [8, 9].

Concerning analysis approach for FAC, in the following are the data parameters selected as distributed:

- thickness of the pipe wall corroded away.

From the viewpoint of probabilistic modelling here, FAC is a somewhat special case as the thickness of the wall corroded away is also the result that is needed for

use in the consequent Markov process analyses. This meaning that in the Markov analysis phase it suffices to sort out from the results the respective degradation states as a function of the operational plant lifetime.

Also described in this section is the development of probabilistic capabilities of the applied fracture mechanics based analysis tool VTTBESIT, which comprises parts developed by the Fraunhofer-Institut für Werkstoffmechanik (IWM), Germany and by VTT [41, 42, 43, 44]. Namely, the new probabilistic distributions developed in this study to the depth and length of initiating SCC cracks were implemented to the VTTBESIT. These were then used in the simulation calculations with the Latin Hypercube Sampling (LHS) application of Monte Carlo simulation ability of the VTTBESIT.

The description of the development and application of probabilistic procedures presented here covers only those carried out in this project. However, this project is more or less a continuation of an earlier VTT project concerning RI-ISI, and for most part by the same VTT project group. In the earlier project parts a number of probabilistic developments for RI-ISI analysis purposes were provided and applied as pilot studies to existing Finnish BWR piping systems, for details see refs. [7, 10, 11].

### 2.2.1 The assessment of probabilistic distributions for sizes of initial cracks induced by SCC

The assessment of probabilistic distributions for depth and length of initial cracks induced by SCC was based on the flaw data from nine Swedish BWR units, see ref. [35]. This data consists of 98 detected SCC cases, all of which are circumferentially oriented cracks at the inner pipe surfaces.

In the assessment of probabilistic distributions for depth and length of initial cracks only those of the above mentioned 98 crack cases were considered in case of which the outer pipe diameters are within the same range as that concerning the analysed piping components, namely from 168 to 273 mm. This limited the number of examined crack data cases to 42. For these cases the data values for detected crack depths vary between 1.5 to 10.0 mm, and for detected crack lengths between 7.0 to 330.0 mm, respectively, while the associated wall thicknesses vary between 7.0 to 52.0 mm. The piping component case application analyses together with the associated input data are described in detail in Chapter 3.

A recursive method based on fracture mechanics and statistical curve fitting was used to calculate the estimates for the probabilistic distributions of the depth and length of cracks that initiate due to SCC during plant operation.

Concerning the estimation of initial crack dimensions in general there are several uncertainties. As the data in the piping degradation databases concerns only detected grown cracks, the initial crack dimensions have to be assessed recursively, which is in several ways an uncertain process. Also, the applicable degradation data is often scarce and of questionable quality, which causes uncertainty as well.

The applied approach to assess the probabilistic distributions of the initial crack sizes from the data of detected cracks is summarized here and described in more detail further below. So, the approach applied here for recursive assessment of the initial sizes for grown SCC induced cracks is such that first the size data concerning detected grown SCC induced cracks, as obtained through screening from the used crack database, is converted to dimensionless form in relation to pipe wall thickness and inner circumference. Then, with fracture mechanics based analyses, the thus obtained data is matched with the assumed initial sizes, the criterion for which here is to correspond to respective mode I stress intensity factor threshold values,  $K_{I,threshold}$ , for SCC initiated cracks. Finally, the thus obtained data is converted to probabilistic form and a suitable reliability distribution function is fitted to it.

The steps of the fracture mechanics and statistical curve fitting based approach concerning the estimation of the probabilistic distributions for SCC initiated cracks are described in the following:

1. Based on the applicable database cases concerning detected grown SCC induced circumferential inner surface piping cracks, see ref. [35], the ages of existing of these cracks are calculated.
2. For recursive fracture mechanics SCC calculations concerning the screened database crack cases the following input data are to be collected/prepared;
  - crack aspect ratio; crack depth divided by half of the crack length,
  - geometry data; pipe outer diameter and wall thickness,
  - material data; for the piping material of austenitic stainless steel, temperature dependent values of yield stress, ultimate stress, elastic modulus and coefficient of thermal expansion,
  - load data; primary membrane and bending stress values calculated with linear beam theory as corresponding to stationary operational conditions with pressure of 7.0 MPa and temperature of 286 °C, which loads were taken from ref. [12],
  - welding process induced residual stresses in the welds; defined according to SINTAP procedure [13], near and in the inner surface this stress component has values of the scale of yield stress in tension, whereas near and in the outer surface of the scale of yield stress in compression, respectively.
3. Performing recursive fracture mechanics SCC calculations concerning the screened database crack cases;
  - deterministic crack size decrease calculations keeping the aspect ratio case specifically as constant; calculations performed with deterministic version of VTTBESIT,
  - in the crack calculations the rate equation for crack depth against time, i.e.  $da/dt$ , was used, for equation background information see ref. [14],
  - the values for temperature, material and environment dependent characterising parameters  $C$  and  $n$  were obtained from ref. [33],
  - crack size decrease calculations backwards in time are performed for each crack case for as long as is the existing age of each case, which was taken to be from the time of detection to the start of operation of the NPP unit in question.
4. Screening of the recursive fracture mechanics SCC calculation results to obtain the crack cases initiated by SCC;

- in principal all initial cracks can be caused by manufacturing; here it is assumed that SCC has taken effect from the start of operation and that all recursively calculated crack cases that are in a fracture mechanics sense small then, i.e. below a few hundred  $\mu\text{m}$  in size, were taken as nucleated by SCC (from impurities, inclusions, small pores), while all other crack cases were taken as manufacturing flaws which have grown in size due to SCC (for the transition in size from microstructurally small cracks to mechanically small cracks, see e.g. ref. [18]),
  - the threshold for crack initiation was assessed in terms of the mode I stress intensity factor ( $K_I$ ) against crack growth speed so that it is approximately such  $K_I$  value in the crack calculation results to the left of which the curve sets itself parallel to horizontal direction, i.e. crack growth speed ceases to be dependent on  $K_I$ , for details concerning the assessment of  $K_I$  threshold values for initial cracks caused by SCC see ref. [25],
  - as a result those crack cases, together with their assessed initial dimensions, that are assumed to be nucleated by SCC are obtained.
5. The estimated initial SCC crack dimensions were divided to subgroups of certain constant sizes;
    - initial crack depth relative to wall thickness; subgroup size of 5 ‰,
    - initial crack length relative to inner pipe circumference; subgroup size of 1 ‰.
  6. The number of cases in each subgroup was calculated separately for assessed initial crack depths and lengths.
  7. The single value probability of each initial crack depth and length subgroup obtained from step 5 was taken as the number of cases in each subgroup, obtained from step 6, divided by the number of all cases.
  8. The distributed probability of each initial crack depth and length subgroup was taken as dividing the single value probabilities obtained from step 7 by the subgroup width.
  9. The exponential function was selected as the form of probabilistic density function for both the estimated initial crack depths and lengths. The justifications for this are the following;
    - due to the non-linear descending slopes of the estimated distributions of initial crack depths and lengths the best fit to them was achieved with the exponential function,
    - the use of exponential function for estimates of initial crack dimension distributions is also recommended in the related relevant literature, see e.g. ref. [15].
  10. In addition to fitting criteria, the quality of the obtained exponential probabilistic distributions was also confirmed through fulfilling the condition that the areas limited from above by each of the two probabilistic density curves, and from left and below by the coordinate axes, equal quite accurately to one. Also note that for relative initial crack depths from 0 to 15 ‰ and for relative initial crack lengths from 0 to 0.5 ‰, respectively, the probability is set to zero.

The fitted exponential probabilistic density functions for estimated SCC induced initial crack depths and lengths are presented as probability against relative crack dimension in Figures 2.2.1-1 and 2.2.1-2.

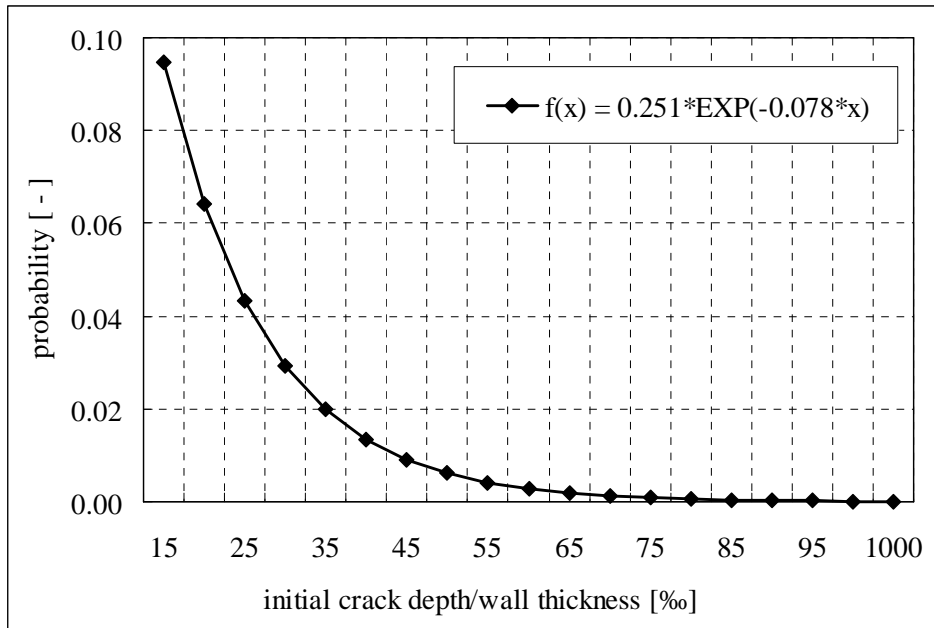


Figure 2.2.1-1. The fitted exponential probabilistic density function for estimated initial crack depths presented as probability against relative initial crack depth. In the legend “f” stands for probability and “x” for relative initial crack depth expressed in [%o]. Note that for relative initial crack depths from 0 to 15 ‰ the probability is set to zero.

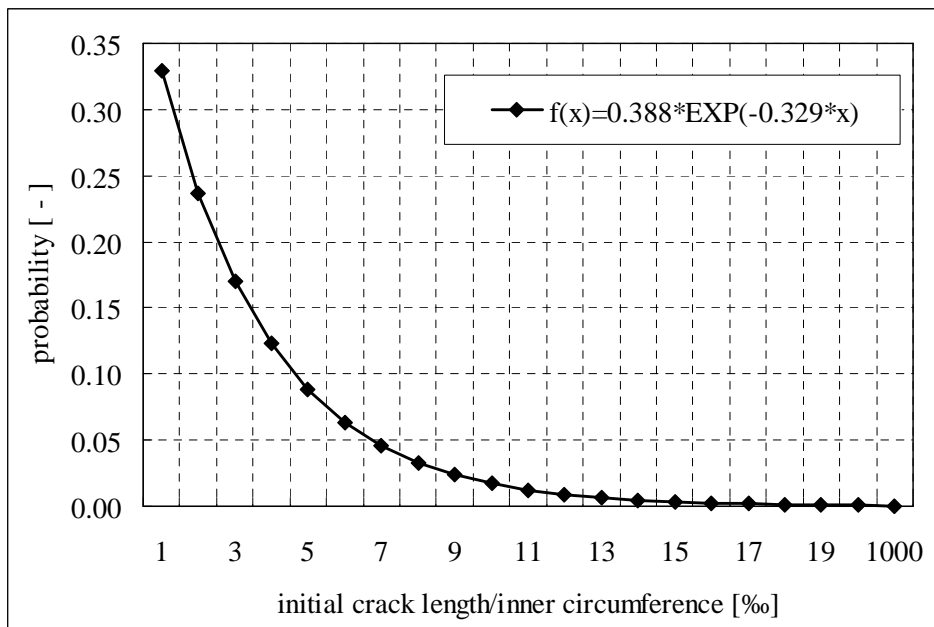


Figure 2.2.1-2. The fitted exponential probabilistic density function for estimated initial crack lengths presented as probability against relative initial crack length. In the legend “f” stands for probability and “x” for relative initial crack length expressed in [%o]. Note that for relative initial crack depths from 0 to 0.5 ‰ the probability is set to zero.



The fitted exponential probabilistic density functions for estimated SCC induced initial crack dimensions were used further in the crack growth simulations so that the values from the distributions are taken at random, and then converted case specifically to physical dimensions, i.e. units of mm.

It was beyond the scope of this study to attempt to create such probabilistic distributions for the initial sizes of SCC induced initial cracks that could be recommended to be used for practical applications in larger scale. Instead the purpose here was more to demonstrate the applied approach and point out the sources of uncertainty/inaccuracy. It is deemed here that with a wider scale of better quality database crack data and with more effort concerning minimising the mentioned uncertainties, more accurate probabilistic initial sizes for SCC induced initial cracks could be obtained, which would also better suit for practical PFM/RI-ISI analysis purposes.

### 2.2.2 Probabilistic FAC model

The FAC process is an extension of the generalized carbon steel corrosion process in stagnant water. In stagnant water, the carbon steel corrosion rate is low and decreases parabolically with time due to the formation of a protective oxide film at the surface. In FAC a thin layer of porous iron oxide forms on the inside surface of carbon steel piping exposed to deoxygenated water. Generally, this layer protects the underlying piping from the corrosive environment and limits further corrosion. However, the magnetite layer may be dissolved at the oxide-water interface and be replaced by new iron oxide formed at the metal-oxide interface, resulting in material removal and thinning of the piping. The corrosion process is strongly influenced by the fluid velocity, chemistry and temperature, piping configuration, and alloy content of the steel [16].

FAC takes place at low flow velocities and the corresponding corrosion rate is constant; this process is called one-phase FAC. The difference between generalized corrosion and FAC is the effect of water flow at the oxide-feedwater interface. A similar corrosion process causes wall thinning of carbon steel piping exposed to wet steam; this process is called two-phase FAC. If the piping is exposed to dry or superheated steam, no FAC takes place; a liquid phase must be present for FAC damage to occur. Corroded surfaces produced by single-phase FAC have a different appearance than those formed by the two-phase FAC [16].

The KWU-KR model [17], which is based on fitting of both detected and experimental data, has been selected for FAC analyses, because of the relevant FAC analysis models it is well documented in the published literature.

The KWU-KR model [17] allows calculating the corrosion rate as a function of Keller's geometry factor, flow velocity, fluid temperature, material chemical composition, fluid chemistry (pH at 25 °C and dissolved oxygen), exposure time, and, in the case of two-phase flow, steam quality. With this model, the pipe wall thickness can be calculated as a function of time. The wall corrosion,  $W_C(t)$  [cm], is the thickness of the pipe wall corroded away, and is given as:



$$W_C(t) = \frac{\Delta\phi_R \cdot t}{\rho_{st}} \quad (2.2.2-1)$$

where  $\Delta\phi_R$  [ $\mu\text{g}/(\text{cm}^2\text{h})$ ] is FAC rate,  $t$  [h] is exposure time and  $\rho_{st}$  [ $\mu\text{g}/\text{cm}^3$ ] is density of steel.

Ref. [17] by Kastner and Riedle is the basis for estimating the FAC rate,  $\Delta\phi_R$ . Once the FAC rate is estimated, the wall thickness as a function of time can be calculated as:

$$W_{pipe}(t) = W_{original} - W_{C,calculated}(t) \quad (2.2.2-2)$$

where  $W_{pipe}(t)$  [cm] is pipe wall thickness at time  $t$  [h],  $W_{original}$  [cm] is original, nominal pipe wall thickness and  $W_{C,calculated}(t)$  [cm] is the calculated thickness of pipe corroded away at time  $t$ .

The corrosion rate,  $\Delta\phi_R$ , is calculated with the following steps.

Using the KWU-KR model, the pH, oxygen content, liquid velocity, geometrical factor, total content of chromium and molybdenum in steel, and operating temperature are needed. The FAC rate is calculated with the following equations [19]:

$$\Delta\phi_R = 6.35 \cdot k_c \cdot \left\{ B \cdot e^{N \cdot w} \cdot \left[ 1 - 0.175 \cdot (pH - 7)^2 \right] \cdot 1.8 \cdot e^{-0.118 \cdot g} + 1 \right\} \cdot f(t) \quad (2.2.2-3)$$

with:

$$\begin{aligned} B &= -10.5 \cdot \sqrt{h} - (9.375 \cdot 10^{-4} \cdot T^2) + (0.79 \cdot T) - 132.5 \\ N &= -0.0875 \cdot h - (1.275 \cdot 10^{-5} \cdot T^2) + (1.078 \cdot 10^{-2} \cdot T) - 2.15 \quad (\text{for } 0 \% \leq h \leq 0.5 \%) \\ N &= (-1.29 \cdot 10^{-4} \cdot T^2 + 0.109 \cdot T - 22.07) \cdot 0.154 \cdot e^{-1.2 \cdot h} \quad (\text{for } 0.5 \% \leq h \leq 5 \%) \end{aligned}$$

where  $\Delta\phi_R$  [ $\mu\text{g}/(\text{cm}^2\text{h})$ ] is the calculated specific rate of material loss,  $k_c$  [ - ] is geometrical factor,  $w$  [m/s] is flow velocity, pH [ - ] is pH value,  $g$  [ $\mu\text{g}/\text{kg}$ ] is oxygen content,  $h$  [total %] is content of chromium and molybdenum in steel,  $T$  [K] is temperature and  $f(t)$  [ - ] is a time correction factor.

Note that the time correction factor,  $f(t)$ , of the FAC rate equation is a function of exposure time in the KWU-KR model [17]. Exploring the behaviour of this factor, it can be shown that  $f(t)$  has a value of 1 in small operating periods and tends to the value of 0.79 for an operating period of  $9.6 \cdot 10^4$  hours (around 11 years). Note that for longer operating periods ( $t \geq 9.6 \cdot 10^4$  hours),  $f(t)$  equals 0.79. The time correction factor is given as:

$$f(t) = C_1 + C_2 \cdot t + C_3 \cdot t^2 + C_4 \cdot t^3 \quad (2.2.2-4)$$

where  $t$  [h] is exposure time,  $C_1 = 9.999934 \cdot 10^{-1}$ ,  $C_2 = -3.356901 \cdot 10^{-7}$ ,  $C_3 = -5.624812 \cdot 10^{-11}$  and  $C_4 = 3.849972 \cdot 10^{-16}$ .

The geometry factor,  $k_c$ , is given by one of the following values [17]:

0.04 for "straight tube"	0.08 for "leaky joints" or "labyrinths"
0.15 for "behind junctions"	0.16 for "behind tube inlet (sharp edge)"
0.23 for "elbow $R/D = 2.5$ "	0.30 for "elbow $R/D = 1.5$ "
0.30 for "in and over blades"	0.52 for "elbow $R/D = 0.5$ "
0.60 for "in branches #2"	0.75 for "in branches #1"
1.0 for "on tubes," "on blade," or "on plate"	

This FAC model was developed in 1980s and, therefore, the further understanding developed since then is not incorporated in the model. The following assumptions are employed in the model. Comments based on the current understanding of the FAC phenomena are also presented, if appropriate, along with each assumption [16]:

1. The model has no restriction on the flow velocity up to the critical velocity with which metal removal takes place by mechanical processes.
2. The FAC rates are insignificant at water temperature greater than 240 °C, and the resulting material losses can be ignored. This assumption is consistent with the current understanding.
3. The lower and upper limits for the cold pH are 7.0 and 9.39, respectively. Note that the typical limits for PWR are 8.5 and 9.5. The model assumes that the corrosion rate is very small (1  $\mu\text{g}/\text{cm}^2/\text{h}$ ) and constant if the pH is greater than 9.39. But the test results show that at higher pH values, the corrosion rate increases with increasing pH value.
4. The oxygen concentration is less than 30 ppb. For higher concentration, the rate is constant and very small. The test results and plant data show that the rate is very small for the oxygen concentration greater than 15 ppb.
5. The chromium and molybdenum content is less than 0.5 wt-%. No material loss takes place if the content is higher. This is conservative because the field data show that there is no material loss if the content is greater than 0.1 wt-%.
6. The model is valid only for operating periods longer than 200 h. Very high losses can occur in the start-up phase.
7. The two-phase FAC model uses the mean velocity in the water film on the inside surface of the piping instead of the velocity of a two-phase fluid. The basic condition is annular flow in two-phase flow. When applying the empirical model for water flow to water/steam flows, the reference velocity used is not the velocity of a two-phase mixture, but the mean velocity in the film of water on the wall of the component,  $W_F$  [m/s]. A simplified equation for this is:

$$W_F = \frac{\dot{m}}{\rho_w} \cdot \frac{1 - x_{st}}{1 - \alpha} \quad (2.2.2-5)$$

where  $\dot{m}$  [ $\text{kg}/(\text{m}^2 \cdot \text{s})$ ] is mass flux,  $\rho_w$  [ $\text{kg}/\text{m}^3$ ] is density of the water at saturation condition,  $x_{st}$  [ - ] is steam quality and  $\alpha$  [ - ] is void fraction.

FAC has been the most destructive corrosion mechanism for high energy carbon steel piping in Light Water Reactors (LWRs). It has caused rupture of both large and small diameter piping carrying either one-phase or two-phase flow. One-

phase FAC has also caused significant wall thinning of carbon steel J-tubes and feed-rings within the recirculating steam generators [16].

In BWRs pipe wall thinning due to FAC has occurred in the feedwater-condensate systems e.g. in straight runs and in elbows [16].

Concerning the analysis approach presented above for FAC, in the following are for PFM analyses the parameters selected as distributed together with the selected reliability distribution functions:

- thickness of the pipe wall corroded away; log-normal probability distribution

The probability distribution for thickness of the pipe wall corroded away is calculated with a probabilistic version of the KWU-KR model [17], taken from ref. [16], and briefly presented in the following.

From the viewpoint of probabilistic modelling here, FAC is a somewhat special case as the probabilistic thickness of the wall corroded away is also the result that is needed for use in the consequent Markov process analyses. This meaning that in the Markov analysis phase it suffices to sort out from the results the respective degradation states as a function of the operational plant lifetime.

To express uncertainty in the KWU model predictions, an adjustment factor is employed. First a multiplicative factor  $E$  is introduced to the deterministic reference model, see equations from (2.2.2-1) to (2.2.2-5). Thus, referring to equation (2.2.2-1), the FAC rate is expressed as:

$$\Delta\phi_R = \Delta\phi_{R,KWU-KR} \cdot E \quad (2.2.2-6)$$

where  $\Delta\phi_R$  [ $\mu\text{g}/(\text{cm}^2\text{h})$ ] is specific FAC rate,  $\Delta\phi_{R,KWU-KR}$  [ $\mu\text{g}/(\text{cm}^2\text{h})$ ] is specific FAC rate as predicted by the KWU-KR model (here deterministic reference model) and  $E$  [ - ] is adjustment factor.

Consequently equation (2.2.2-1) can be expressed as:

$$W_{C,calculated}(t) = \frac{E \cdot \Delta\phi_{R,KWU-KR} \cdot t}{\rho_{st}} \quad (2.2.2-7)$$

Thus the actual specific FAC rate can be considered to be the product of its deterministic reference model prediction and an adjustment factor  $E$  which accounts for the inadequacy of the calculated value.

The next procedure step is to divide the examined range of FAC rates [ $\mu\text{g}/(\text{cm}^2\text{h})$ ] to four specified regions as follows:

- Region I; 1 – 10
- Region II; 10 – 50
- Region III; 50 – 200
- Region IV; 200 – 2000

FAC rates outside the above presented four regions are assessed to occur in NPP piping systems very seldom, if at all.

The probability distribution function for the adjustment factor  $E$  is assumed as log-normal with parameters  $\mu_E$  and  $\sigma_E$ , i.e. scale and shape parameters, respectively. The log-normal distributions for the adjustment factor  $E$  for the four FAC rate regions are presented in Table 2.2.2-1.

It is recommendable to compare the obtained reliability distributions for FAC rate to data both in international degradation databases and the plant specific degradation database.

*Table 2.2.2-1. The log-normal distributions for the adjustment factor  $E$  for the four FAC rate regions.*

<b>Parameter</b>	<b>Region I</b>	<b>Region II</b>	<b>Region III</b>	<b>Region IV</b>
$\mu_E$	0.33	-1.17	-0.72	-2.03
$\sigma_E$	1.17	1.15	1.04	1.65
5 <sup>th</sup> percentile	0.20	0.05	0.09	0.009
50 <sup>th</sup> percentile	1.39	0.31	0.49	0.13
95 <sup>th</sup> percentile	9.47	2.06	2.66	1.99
Mean	1.43	0.61	0.83	0.51
Error factor	6.83	6.62	5.46	14.99

### **3 Comparative pipe leak/rupture probability analyses of the OL1 piping system 321**

#### **3.1 Overview of the piping system and its division to segments**

The main task of the OL1 Shut-down cooling system 321 is the cooling of the reactor when it is shut down during fuel change or during cold shutdown. When the head of the reactor pressure vessel (RPV) is to be opened, system 321 feeds water to the Flange cooling system 326. During the replacement of fuel elements system 321 and Pool water system 324 cool the fuel element storage pools, reactor pool and the storage pools of RPV internals. During all operational conditions system 321 feeds water to the Reactor water clean-up system 331, after which it returns this water to the RPV. Main part of the water is returned to the Feed water system-reactor 312 and the rest through the Hydraulic scram system 354 to the primary circuit. Together with the RPV system 321 forms a closed circuit. In the containment building lead-ins there are in suction and pressure lines both internal and external isolation valves, in addition to which the internal isolation valves are in series with maintenance valves. Only one of the two pumps is in service during normal operation. Heat exchangers 321 E1 and E2 are in operation only during the shutdown and the fuel change. The consequence of losing the integrity of system 321 would be a LOCA either inside or outside the containment. The system 321 contains four pipe lines that penetrate the containment, each of which contains an isolation valve both inside and outside the containment [2].

The total length of the piping components of the system 321 is approximately 400 m, and the number of circumferential welds joining them is several hundreds. Most piping components run in horizontal or vertical directions, and a minor part of the piping components runs in oblique directions.

The segmentation is based on four main criteria [2]:

- isolation actions with which the consequences of a leak can be restricted,
- degradation mechanisms in question,
- direct consequences, and
- indirect consequences.

The location of the leak holds significance for the plant response, and through that to systems the use of which will be prevented as a consequence of the leak. Another criterion for this division is the possibility to isolate the leak using isolation valves.

All in all the system 321 is divided to 20 segments, see ref. [2].

#### **3.2 Prevailing degradation mechanisms and selection of the analysed piping welds**

The most notable degradation mechanisms affecting the system 321 are assumed to be stress corrosion cracking (SCC) and thermal fatigue in the mixing points.

There are also several segments in the system 321 which are assumed to be affected by no degradation mechanism.

A pipe leak/rupture probability and RI-ISI analysis has been performed earlier as a pilot study to the OL1 system 321 by mostly the same researchers, see ref. [7]. In that study 16 piping welds were analysed with PFM and RI-ISI applications developed mainly in VTT. These analysed welds cover all those segments in the system 321 being susceptible to SCC and thermal fatigue in the mixing points.

In the analyses here the purpose is in case of SCC to compare the effect of certain modifications in the defined probabilistic input data to the PFM analysis results, i.e. pipe leak/rupture probabilities. Thus it sufficed to select a smaller number of piping welds than covered in ref. [7] for PFM reanalyses here.

Here 5 piping welds from the earlier study [7] were selected for PFM reanalyses. The compared feature is the impact of different probabilistic distributions for initial crack sizes caused by SCC on leak/rupture probability results.

All reanalyzed 5 piping welds are located outside the containment in the reactor building. Here the naming system of the analysed piping welds in the earlier study [7] has been preserved. All 16 piping welds analysed in ref. [7], and thus including those 5 piping reanalysed in this study, are presented in Table 3.2-1. The reanalysed 5 welds are emphasized with blue colour and bold font.

*Table 3.2-1. The 16 piping welds analysed in ref. [7], and thus including those 5 piping reanalysed in this study. The reanalysed 5 welds are emphasized with blue colour and bold font.*

<b>Piping weld</b>	<b>Degradation mechanism</b>
3-1-2--1	SCC
4-1-0--2	SCC
<b>4-1-0--3</b>	<b>SCC</b>
<b>4-1-0--4</b>	<b>SCC</b>
4-1-0--5	SCC
<b>4-1-0--6</b>	<b>SCC</b>
4-1-3--7	SCC
<b>4-1-3--8</b>	<b>SCC</b>
4-3-0--9	thermal fatigue
4-3-2--10	thermal fatigue
4-4-0--11	thermal fatigue
4-5-0--12	thermal fatigue
<b>4-8-0--13</b>	<b>SCC</b>
4-8-0--14	SCC
4-8-0--15	SCC
4-8-0--16	SCC

### 3.3 Input data for PFM analyses

The geometry, material and load data of the piping system 321 presented here are taken from the design drawings, from Section II of the ASME code [27] and from ABB ATOM Materialhandboken [28]. On the behalf of geometry data, the presented dimensions are approximate. However, accurate values were used in the analyses. The mechanical and thermal material property values are temperature dependent, and presented below only for temperatures of 20 °C and 286 °C, as these are the only temperatures necessary to cover in the analyses here.

As the input data used in the PFM analyses here has already been mostly presented in the earlier study [7] concerning the OL1 piping system 321, it is only briefly summarised here.

The geometry and material properties used in the PFM analyses of the 5 considered piping welds of the system 321 are presented in Tables 3.3.1 to 3.3.3. The only considered load case is stationary operational conditions. Also welding process induced residual stresses in the welds were considered in the analyses.

*Table 3.3-1. The geometry and materials of the analysed piping welds of the system 321.*

Piping weld	Material	Outer diameter [mm]	Wall thickness [mm]
4-1-0--3	376 TP 304	273	21
4-1-0--4	376 TP 304	219	18
4-1-0--6	376 TP 304	168	14
4-1-3--8	376 TP 304	219	18
4-8-0--13	376 TP 304	168	14

*Table 3.3.2. Mechanical material properties of steel SIS2333 as a function of temperature. These values can be used for steel 376 TP 304, see ref. [28].*

Temperature [°C]	Young's modulus [GPa]	Yield strength [MPa]	Tensile strength [MPa]
20	201	210	515
286	176	125	383

*Table 3.3.3. Thermal material properties of steel SIS2333 as a function of temperature. These values can be used for steel 376 TP 304, see ref. [28].*

Temperature [°C]	Thermal expansion [ $10^{-6}/K$ ]	Thermal conductiv. [W/mK]	Specific heat [J/kgK]
20	17.0	15.0	440.0
286	18.5	18.6	537.2

The type of the piping welds is taken as Shielded Metal Arc Welding (SMAW). According to ref. [29], when the base material of the pipe is austenitic stainless steel and temperature is 288 °C, the fracture toughness data for this welding type are:  $K_{Ic} = 182 \text{ MPa}\cdot\sqrt{\text{m}}$ ,  $J_{Ic} = 168 \text{ kJ/m}^2$ , and for the base material:  $K_{Ic} > 350 \text{ MPa}\cdot\sqrt{\text{m}}$ ,  $J_{Ic} > 620 \text{ kJ/m}^2$ .

The experimentally defined parameter values used in the crack growth equations and which characterise the material properties as a function of temperature and environment are presented in Table 3.3.4, in which  $K_I$  is the mode I stress intensity factor (SIF),  $a$  is the crack depth and  $t$  is time.

*Table 3.3.4. Values of parameters  $C_{SCC}$  and  $n_{SCC}$  used in the SCC equation for the considered material. The dimensions used in the crack growth equation are:  $[da/dt] = \text{mm/year}$ ,  $[K_I] = \text{MPa}\cdot\sqrt{\text{m}}$ , see ref. [33].*

Material	$C_{SCC}$	$n_{SCC}$	Environment
376 TP 304	$1.42 \cdot 10^{-04}$	3.00	water

Under operational conditions the values of internal pressure and temperature of the fluid are 7.0 MPa and 286 °C, respectively, see ref. [12].

The axial membrane stress  $\sigma_a$  caused by internal pressure was calculated with the following equation [34]:

$$\sigma_a = \frac{p \cdot (D/2 - t)}{2 \cdot t} \quad (3.3.1)$$

where:  $p$  [MPa] is pressure,  
 $D$  [mm] is outer diameter, and  
 $t$  [mm] is wall thickness.

The bending stresses caused by dead weight of the pipe and fluid (water) were calculated with the beam theory equations.

The values of the welding process induced axial residual stress distribution in the weld centre line and heat affected zone (HAZ) were assumed according to recommendations by Brickstad and Josefson as [21], written here in a slightly modified form:

$$\sigma_{a,resid} = 228, \quad \text{when } 0 < t \leq 7 \text{ mm} \quad (3.3.2)$$

$$\sigma_{a,resid} = 297 - 9.88 \cdot t + \left( 19.76 - \frac{594}{t} \right) \cdot x, \quad \text{when } 7 < t \leq 25 \text{ mm} \quad (3.3.3)$$

where  $\sigma_{a,resid}$  [MPa] is the axial weld residual stress,  $x$  [mm] is the radial coordinate through the wall thickness having origin at inner surface, and  $t$  [mm] is the wall thickness.

This is the same welding residual stress distribution that was used in the earlier study [7], and was selected for analyses presented here in order to keep the reanalyses fully comparable besides the only differing input data, which are the above mentioned probabilistic distributions for the sizes of initial cracks caused by SCC.



All reanalysed cases are circumferentially oriented semi-elliptic surface cracks in the piping component welds. The probabilistic distributions for the sizes of initial cracks caused by SCC developed in this study are presented in Section 2.2.1.

Due to the orientation of the reanalysed piping crack cases and that only mode I loading is considered, only stresses perpendicular to crack planes are considered, these being axially oriented stress components in the piping geometry.

In the earlier RI-ISI pilot study [7] a somewhat straightforward procedure was followed when assessing the probabilistic sizes for initial cracks caused by SCC. The same SCC crack database [35] was used then as is used in this study.

In short the approach for recursive assessment of initial sizes for grown SCC induced cracks applied in ref. [7] is as follows:

- in relation to pipe wall thickness and inner pipe circumference convert to dimensionless form the size data concerning grown SCC induced cracks as obtained through screening from suitable/applicable available cracking database,
- by offset lower thus obtained data in terms of relative crack depth and length, criterion for sought initial sizes being to have the mean value of the lowered data to coincide the size corresponding to a previously selected realistic value,
- convert the thus obtained data to probabilistic form and fit a suitable reliability distribution function to it.

This procedure to assess the initial sizes of cracks caused by SCC is partly similar to the more advanced and realistic one applied here, see Section 2.2.1. The main difference between the two procedures is that in the latter one presented and used in this study the assessment of initial crack sizes is based on fracture mechanics and to a crack growth equation that has been correlated to crack growth propagation rate data from a considerable number of laboratory results. It is deemed that the procedure presented here is more realistic than the one developed earlier, see ref. [7].

### 3.4 Crack growth simulations

In this study the purpose is to improve the probabilistic distributions for initial crack sizes caused by SCC as well as to compare the effect of this input data to the PFM analysis results, i.e. pipe leak/rupture probabilities, obtained in this study and in the earlier analyses with more crudely defined probabilistic initial crack size distributions, see ref. [7].

As there was no actual degradation/failure data available concerning the analysed piping system 321, it was not possible to quantify leak/rupture probabilities of the piping components with statistical methods. Hence this was carried out by performing PFM analyses with a modified version of the analysis code VTTBESIT, developed by the Fraunhofer-Institut für Werkstoffmechanik (IWM), Germany and by VTT [41, 42, 43, 44]. With the probabilistic VTTBESIT it is possible to perform Latin Hypercube Sampling (LHS) simulations of crack growth. Originally VTTBESIT was capable only for deterministic fracture

mechanics based crack growth analyses. A brief description of the main characteristics of VTTBESIT is presented in Section 3.4.3.

The input data needed in the VTTBESIT analyses was discussed and presented in Sections 2.2.1 and 3.3.

### 3.4.1 Analysed cases

The reanalysed piping welds were chosen from those segments which are assumed to be susceptible to SCC, see ref. [2]. All in all 5 piping welds were chosen to be analysed. All of them are located outside the containment in the reactor building. All of them were analysed for SCC. All reanalysed piping welds together with some relevant characteristic data are listed in Table 3.4.1-1. Here the naming system of the analysed piping welds in the earlier study [7] has been preserved.

*Table 3.4.1-1 The 5 piping welds covered in the PFM reanalyses together with some relevant characteristic data [2, 20].*

<b>Piping weld</b>	<b>Analysed material</b>	<b>Outer diameter [mm]</b>	<b>Wall thickness [mm]</b>	<b>Degradation mechanism</b>	<b>Inspection interval *) [years]</b>
4-1-0--3	376 TP 304	273	21	SCC	3
4-1-0--4	376 TP 304	219	18	SCC	10
4-1-0--6	376 TP 304	168	14	SCC	none
4-1-3--8	376 TP 304	219	18	SCC	3
4-8-0--13	376 TP 304	168	14	SCC	none

\*) Inspection interval data is taken from the system 321 study by the Finnish Radiation and Nuclear Safety Authority (STUK) [20].

Here only the older of the two present NPP units of TVO, namely OL1, was studied. OL1 started operation in 1978 [36]. The planned time of operation of the plant is assumed as 60 years.

### 3.4.2 Analysis approach and crack growth equations

The applied PFM analysis approach is briefly described in this section. In short it consists of collecting sufficient amount of input data, some of which are result data calculated with one or several procedures/analysis tools, then assembling this input data in certain ways, and then inserting it to crack growth simulations, which are finally performed with a probabilistic version of the earlier mentioned VTTBESIT code.

As discussed earlier in this report, the input data needed in the PFM analyses are collected from many sources, and have several forms i.e. deterministic single values and probabilistic distributions.

There are several ways of calculating the stresses caused by both time dependent and independent loads, which stresses are part of the input data needed in the PFM analyses. Depending on the complexity/simplicity of the considered

geometries, support conditions and loads, and of the variation of the latter as a function of time, advanced numerical analysis tools, such as those based on Finite Element Method (FEM), may have to be used, or in the most simple case straightforward analytical handbook equations may suffice. Stress analysis tools with the level of sophistication falling somewhere in between these two mentioned extremes exist as well.

The support conditions of piping components are most often quite flexible, the geometry of the piping components is also most often quite simple, symmetric and regular and the loads they are exposed are mainly symmetric as well. Due to this it was not necessary to use an advanced FEM code to solve the time dependent/independent stress distributions the examined piping section walls experience under the considered load case stationary operational conditions.

As for the degradation mechanism analysed here, namely SCC, it is mainly influenced by the stationary operational conditions, during which loads are taken mostly as time independent, but also by some global transient load cases. However, their overall contribution to the loading conditions is minor, since during a typical plant year their summed up duration time is considerably shorter than that of the stationary operational conditions. Thus it is typical to omit the transient load cases from the SCC analyses. For stationary operational conditions considered here, suitable handbook equations to calculate the stress distributions over piping section walls were available, see Section 3.3. It was also necessary to include in the SCC analyses the welding process induced residual stresses, which were estimated according to equations in reference [21].

All analysed locations were circumferential piping welds, and only circumferential surface crack postulates were considered.

As no degradation data concerning the analysed piping system 321 of TVO was available, to a reasonable extent applicable crack data taken from reference [35] was used instead. Based on this data, probabilistic distributions were estimated both for the depth and length of the initial cracks caused by SCC. An estimate for the formation frequency of initial cracks was also taken from reference [35].

### **Probabilistic analysis capabilities of analysis code VTTBESIT**

All crack growth simulations were carried out with a probabilistic version of fracture mechanics based analysis code VTTBESIT [41, 42, 43, 44]. New code development work was performed within this study, as mentioned in Section 2.2.

The analysis procedure of the probabilistic version of VTTBESIT is described in the following:

- reading of the deterministic input data,
- random picking of certain input data parameters from the specified distributions; 1) SCC; probability distributions for initial crack depth and length, 2) fatigue; probability distributions for initial crack depth, length and for load cycle frequency,
- crack growth analysis; the amount of crack growth in each time step is calculated from the respective crack growth equation  $\Rightarrow$  the ending criterion of the analysis is that crack depth reaches the outer pipe surface,

- for each analysed circumferential piping weld at least 1000 separate simulations with LHS procedure are calculated, and for each of these values of the above mentioned distributed input data parameters/variables are picked at random from the respective probabilistic distributions,
- the degradation state to which the crack has grown is calculated for each year of the estimated time of operation and for each simulation  $\Rightarrow$  these results are used in the consequent Markov system probabilistic degradation analyses performed with a Matlab application developed in the project.

### Crack growth equation for SCC

SCC is a localised non-ductile progressive failure mechanism that occurs only in case the following three conditions are fulfilled simultaneously, see ref. [38]:

- the stress around the crack-tip is tensile,
- the environment is aggressive,
- the material is susceptible to SCC.

SCC is also a delayed failure process. That is, cracks initiate and propagate at a slow rate until the stresses in the remaining ligament of metal exceed the fracture strength. The sequence of events involved in the SCC process is, according to ref. [39], usually divided into three stages:

- crack initiation,
- steady state crack propagation,
- final failure.

The fracture mechanics based crack growth equation used in the analyses, which depicts intermediate (stage 2) SCC, is according to refs. [14 ,40]:

$$\frac{da}{dt} = C_{SCC} \cdot K_I^{n_{SCC}} \quad (3.4.2-1)$$

where  $t$  is the time, and  $C_{SCC}$  and  $n_{SCC}$  are constant value parameters characterising the material properties as a function of temperature and environment. The values of these constants were given in Table 3.3.4 in Section 3.3.

#### 3.4.3 Analysis code VTTBESIT

The probabilistic fracture mechanics based crack growth simulations were performed with the analysis code VTTBESIT. This analysis code comprises parts developed by the Fraunhofer-Institut für Werkstoffmechanik (IWM), Germany and by VTT [41, 42, 43, 44].

The stress intensity factor calculations are performed using the program BESIT60 developed by IWM. It is based on the weight function method and on the influence function method. Solutions are provided for "infinite" and semi-elliptical crack cases in plates and cylinders. The theoretical background and analysis procedures of BESIT60 are presented in refs. [41, 42, 43, 44].

VTTBESIT uses the BESIT60 program code as a pure stress intensity factor computing subroutine and applies the results as starting values for crack growth assessments.

With the VTTBESIT software it is possible to quickly compute the stress intensity factors along the crack front and crack growth. The analysis code treats only the mode I loading in which the direction of the loading is perpendicular to the crack surface (crack opening mode) [43].

Material and geometry data needed for the computation are given through a graphical interface. The same data can also be given in a text file format. Loading data, in form of stress distributions through the component wall, are given in a separate file. Loading data can be given as a function of time either in Cartesian or polar co-ordinates [43].

In the VTTBESIT analyses crack growth is calculated for the defined initial crack postulates. Two crack growth models are provided in the analysis code: Paris-Erdogan equation for fatigue induced crack growth, see ref. [37], and rate equation for SCC, here equation (3.4.2-1).

Thus, besides SIFs, VTTBESIT results include also the dimensions of the growing crack as a function of load cycles in case of fatigue and as a function time in case of SCC. The analysis code writes the results in a separate file.

The code development works performed in this study include:

- for SCC analyses, the random picking of initial crack depths and lengths from the developed new probabilistic distributions for SCC induced initial cracks.

#### 3.4.4 Results from VTTBESIT analyses

A description of the results obtained from VTTBESIT analyses is presented in this section. As the amount of results is large, and since in this study their nature is more as intermediate since they are merely used as input data in the consequent Markov system analyses, the numerical presentation of them is omitted here. Instead, the various types of results obtained from the analyses with the probabilistic version of VTTBESIT are described here, and the actual analysis results are only summarised briefly.

As mentioned earlier, with VTTBESIT software it is possible to quickly compute the mode I SIFs along the crack front as well as crack growth. In this study semi-elliptical surface crack postulates are examined. For those the code presents the results are as a function of time at various locations in the crack front:  $\phi = 0^\circ$  (first crack mouth),  $\phi = 30^\circ$ ,  $\phi = 60^\circ$ ,  $\phi = 90^\circ$  (crack tip),  $\phi = 120^\circ$ ,  $\phi = 150^\circ$ , and  $\phi = 180^\circ$  (second crack mouth), where the origin of the angular crack front location parameter  $\phi$  is in the midpoint of the symmetry axes of the half-elliptical crack [43].

In case of SCC the crack growth results are presented as a function of time. More precisely, the presented crack growth results are the crack dimensions, i.e. depth

and length, in each time step, taken from the same crack front locations as the SIF results.

In addition to the above mentioned results, the probabilistic version of VTTBESIT calculates also the various states of degradation of growing cracks. More precisely, for each analysed location 1000 LHS calculations are performed, and for each of these the state of degradation is presented for each year of the given time of operation. In this study the time of operation was assumed as 60 years. Thus for each analysed location, i.e. piping weld, there are  $1000 \cdot 60 \cdot 2 = 120\,000$  result data entries.

As for the degradation analysis results, they are quite similar for the 5 analysed piping weld cross-sections. This is an expected outcome, as SCC is the considered degradation mechanism in all cases and the loads as well as the overall conditions the covered welds are exposed to are very similar. The dimensions of the analysed piping weld cross-sections differed to some extent, though, with the outer diameter altering from approximately 160 to 273 mm, and the wall thickness from approximately 14 to 21 mm. The analysis results seem quite realistic too, for instance many of the SCC cases fail in the same plant age as have been encountered in BWR plants. However, for VTTBESIT analyses with the new probabilistic distributions for initial cracks induced by SCC the results concerning one piping weld, namely 4-1-0--3 (see Table 3.4.1-1), differ considerably from all other results. Namely, only extremely few of the performed 1000 LHS simulations for this case resulted with crack growing through wall. This is mostly explained due to this piping weld having the thickest wall of the analysed cases, being approximately 21 mm. If the analyses would have been continued past the assumed planned operational lifetime of 60 years, it is likely that more simulations would have ended up with crack growing through wall.

In this study the purpose is also to compare the effect of the two sets of probabilistic distributions for initial sizes of cracks nucleated by SCC during operation to the PFM analysis results by applying those probabilistic distributions developed in this study and those in the earlier study, see ref. [7]. The former and more advanced probabilistic initial crack distributions are based on fracture mechanics and statistical fits, whereas the latter and more crudely defined ones to simple crack size decrease by offset and statistical fits. The probabilistic sizes of SCC induced initial cracks are according to the new distributions considerably smaller than those according to the earlier study, see ref. [7]. This is consequently reflected in the PFM analysis results, as much fewer simulations end up with crack growing through wall with the former distributions than with the latter ones, the relative difference being of the scale of one hundred.

## 3.5 Pipe component leak/rupture probability analyses

### 3.5.1 Analysis approach

The pipe component leak/rupture probability analyses were carried out with a Markov system based application, implemented with Matlab code. Here the same version of this Markov application was used as that developed during the previous



phase of this project, for details, background theory and procedure description, see ref. [11].

The first step in analysing the PFM simulations with the developed discrete Markov system application is to create a so called degradation matrix. The elements  $a_{ij}$  of the matrix are state transition probabilities, indicating the probability that the crack, belonging to state  $i$  will end up to the state  $j$  within a time step. In our analyses, the time step is one year. The states are defined in the Table 3.5.1 below.

Table 3.5.1. Markov system states.

State	Crack depth	Description
0	0	New piping section falls into this category.
1	0-1mm	Small flaw - very unlikely to detect
2	1mm-50% of wall thickness	Progressed crack in the segment. Possibility of detection, but no repair.
3	50-99% of wall thickness	Grown crack. Possibility of detection and then segment is repaired.
4	99%-<100%	Leak-before-break. Repaired if detected.
5	100%	Rupture.

The degradation matrices were calculated from the simulation runs.

The second step is to form a vector describing the discretised distribution of initial crack size, and calculate the failure probabilities using the degradation matrix and this vector. In the first analysis, inspections are not taken into account. In such a case, the crack size distribution after  $n$  years is obtained simply by multiplying the initial crack size vector by the degradation matrix  $n$  times.

The third step is to analyse the failure probabilities when in-service inspections are taken into account. Inspection matrices are used to simulate the effects of periodical inspections on the piping conditions. While the degradation matrix has probabilities greater than zero only for transitions to higher states, inspection matrix has transitions only to lower states. It is beyond the scope of this study to evaluate the inspection work with other than simple detection probabilities for leaks and fractures. The inspection matrix used in this study, as taken from ref. [7], is:

$$M_{ins} = \begin{bmatrix} 1 & 0 & 0 & 0 & 0 & 0 \\ 0 & 1 & 0 & 0 & 0 & 0 \\ 0 & 0 & 1 & 0 & 0 & 0 \\ 0.9 & 0 & 0 & 0.1 & 0 & 0 \\ 0.9 & 0 & 0 & 0 & 0.1 & 0 \\ 0 & 0 & 0 & 0 & 0 & 0 \end{bmatrix} \quad (3.5.1)$$

The matrix element  $a_{kk}$   $k = 0 \dots 5$  on the diagonal represent the non-detection probability of a flaw. State 0 is a flawless segment, state 1 includes cracks small enough not to be detected and state 2 includes detectable cracks that are small

enough not to be repaired. In the case of states 3 and 4 (flaws exceeding 50 % of the wall thickness and leaks), it is assumed that if detected (probability of 0.9) a flaw or leak is repaired implying a transition to the flawless state (0).

### 3.5.2 Results from the Markov application analyses

The pipe component leak/rupture probability analysis results for the considered 5 piping welds are presented and discussed in the following.

Each weld is at a flawless state in the analyses here when the operation of the NPP is started - year 0 in this study. When the NPP is used, the yearly rupture probabilities start to climb towards a steady-state rupture probability. This means that as the time advances, the significance of the initial state slowly decreases.

As mentioned earlier, the only considered degradation mechanism is SCC, and the sizes of the initial cracks are taken at random from the probabilistic distributions developed here for the SCC induced initial cracks. The effect of these for the pipe leak/rupture probabilities are compared to the respective results calculated with corresponding more crude probabilistic distributions developed in the earlier study, see ref. [7].

The pipe component rupture probability analysis results for the considered 5 piping welds are presented in Figures 3.5.2-1 to 3.5.2-5. In the following Table 3.5.2-5 are presented the meanings concerning the result graph colours and line types used in the Figures 3.5.2-1 to 3.5.2-5.

*Table 3.5.2-5. The meanings concerning the result graph colours and line types used in Markov analysis result Figures 3.5.2-1 to 3.5.2-5.*

<b>Notation</b>	<b>Green colour</b>	<b>Blue colour</b>	<b>Continuous line</b>	<b>Dashed line</b>	<b>Dash-dotted line</b>
<b>Meaning</b>	results for new developed probabilistic size distributions for SCC induced initial cracks	results for earlier developed probabilistic size distributions for SCC induced initial cracks, see ref. [7]	no inspections	10 year inspection intervals	5 year inspection intervals



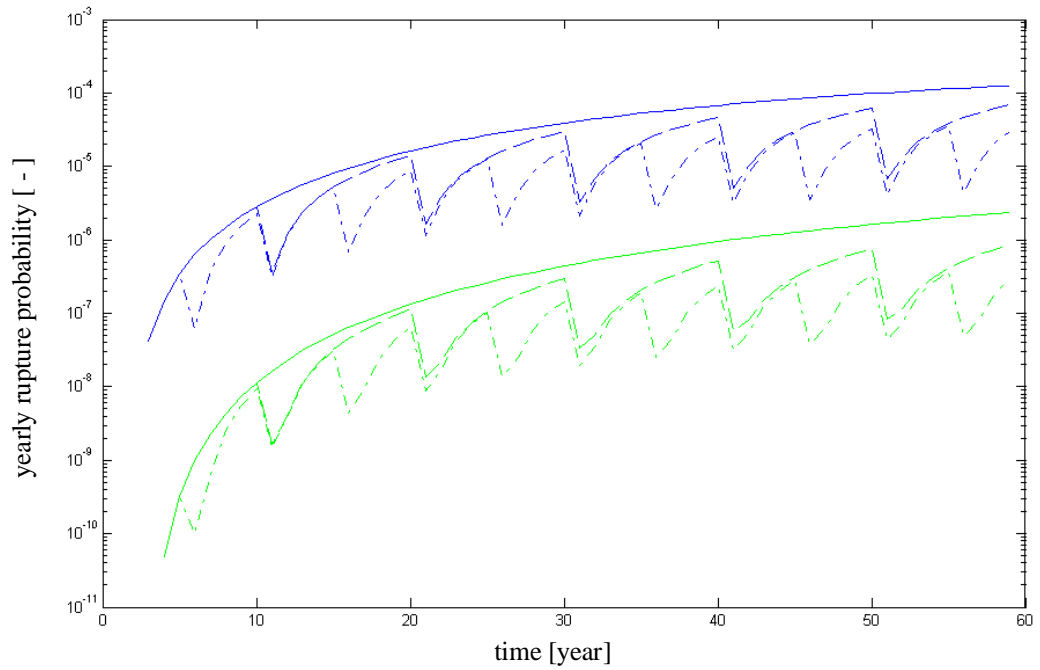


Figure 3.5.2-1. The yearly rupture probability analysis results for piping weld 4-1-0-4 as a function of operational lifetime. For meanings of used colours and line types: see Table 3.5.2-5.

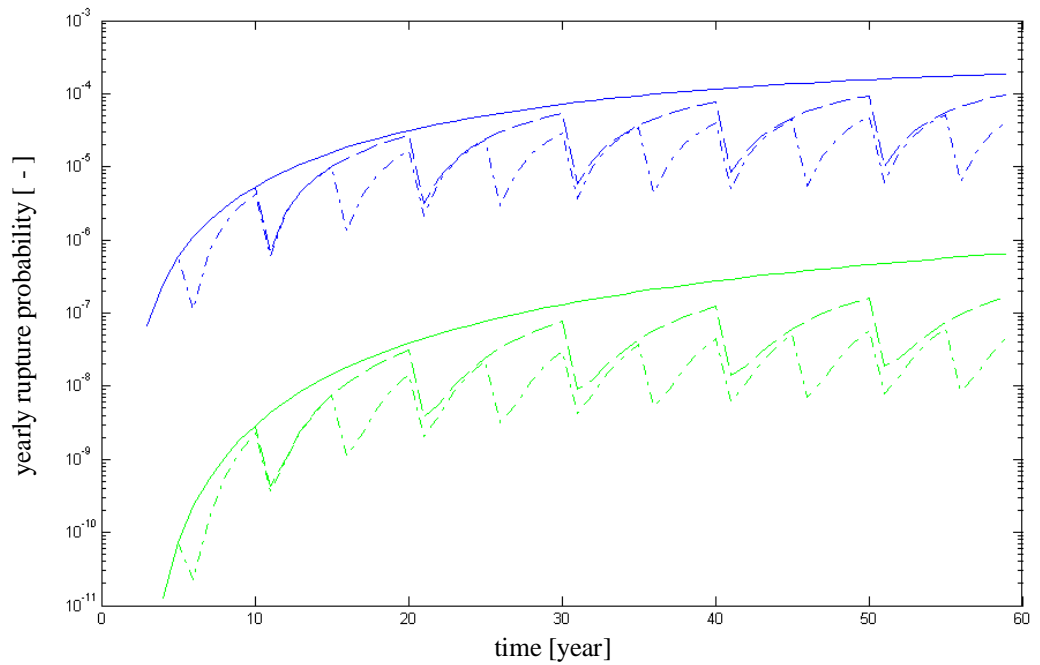


Figure 3.5.2-2. The yearly rupture probability analysis results for piping weld 4-1-0-6 as a function of operational lifetime. For meanings of used colours and line types: see Table 3.5.2-5.

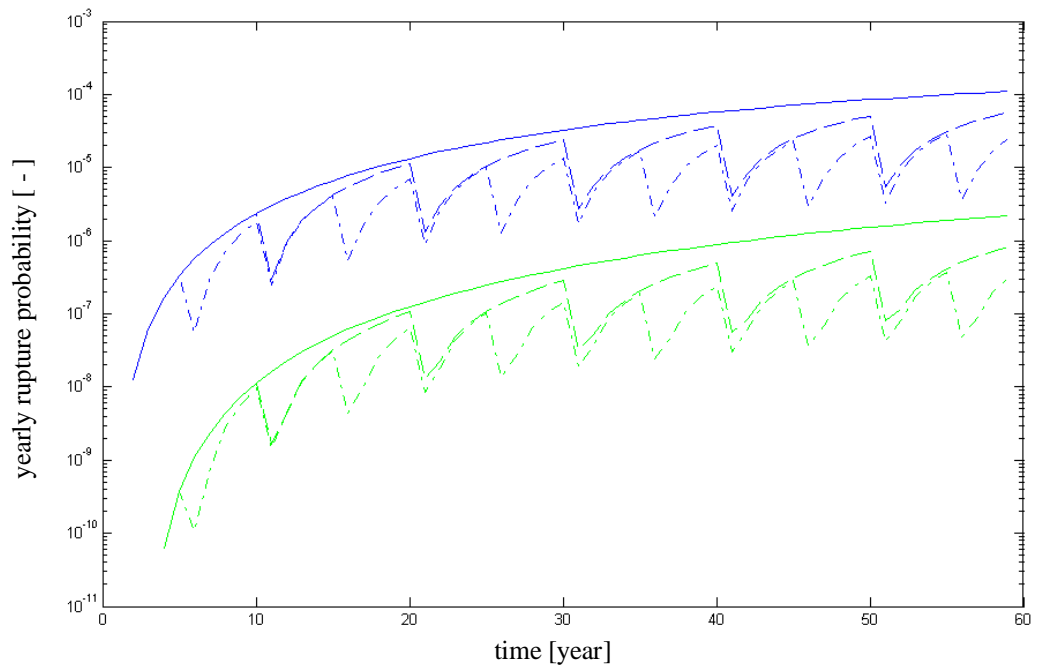


Figure 3.5.2-3. The yearly rupture probability analysis results for piping weld 4-1-3--8 as a function of operational lifetime. For meanings of used colours and line types: see Table 3.5.2-5.

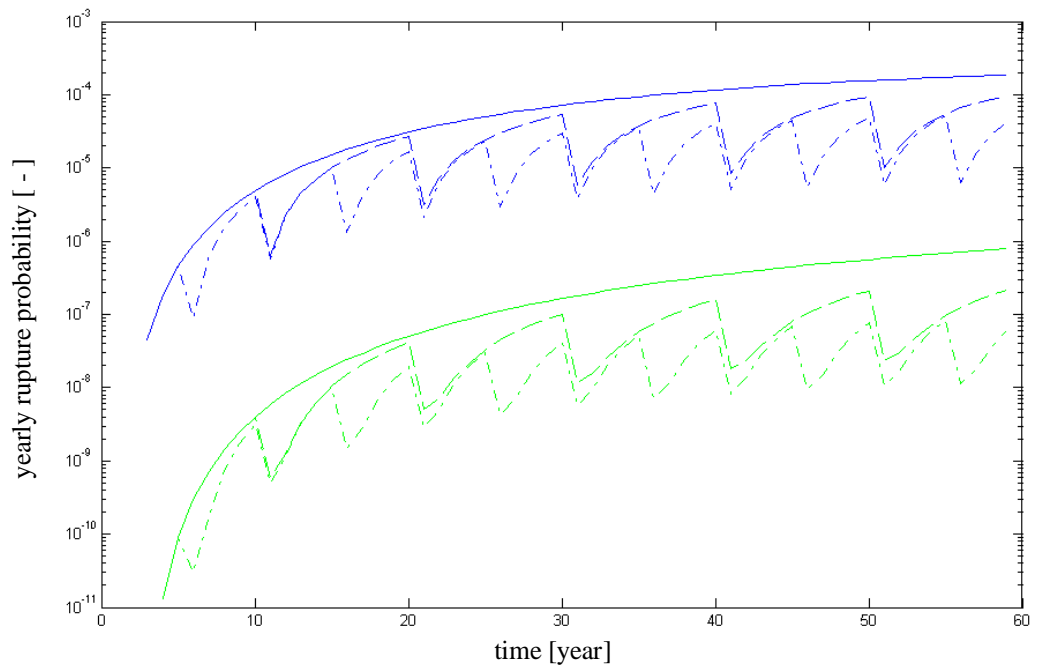
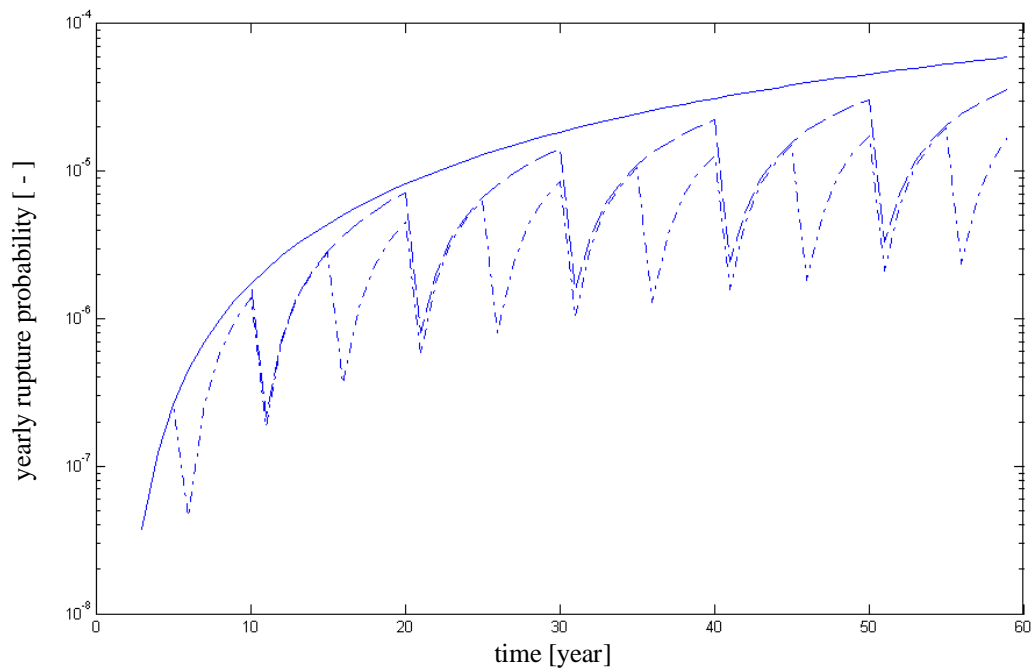


Figure 3.5.2-4. The yearly rupture probability analysis results for piping weld 4-8-0--13 as a function of operational lifetime. For meanings of used colours and line types: see Table 3.5.2-5.



*Figure 3.5.2-5. The yearly rupture probability analysis results for piping weld 4-1-0--3 as a function of operational lifetime. For meanings of used colours and line types: see Table 3.5.2-5.*

It can be noticed from Figures 3.5.2-1 to 3.5.2-5 that depending on the weld the assumed operational plant lifetime of 60 years is enough for the welds to approximately reach steady-state. The measure used for pipe degradation in this study is the average yearly rupture probability.

The effects of the inspections are seen as saw-type deviations in the yearly rupture probability. Using this measure the rupture probability decreasing effects of the inspections are clear.

All in all the yearly rupture probability results are mostly quite similar for the 5 analysed piping weld cross-sections. This is an expected outcome, as SCC was the considered degradation mechanism in all cases and the loads as well as the overall conditions the covered welds are exposed to are very similar. However, for VTTBESIT analyses with the new probabilistic distributions for initial cracks induced by SCC the results concerning one piping weld, namely 4-1-0--3 (see Table 3.4.1-1), differed considerably from all other results. Namely, the rupture probability results for input data case with the new probabilistic distributions for sizes of SCC induced initial cracks were practically zero, which can be noticed in their absence from the Figure 3.5.2-5. This is mostly explained due to this piping weld having the thickest wall of the analysed cases, being approximately 21 mm.

In this study the purpose is also to compare the effect of the two sets of probabilistic distributions for initial sizes of SCC induced cracks during operation to the pipe rupture probabilities. As mentioned earlier, these probabilistic initial crack sizes are according to the new distributions developed in this study considerably smaller than those according to the earlier study, see ref. [7]. For instance for the former distributions the mean crack depth is approximately 300

$\mu\text{m}$ , whereas for the latter ones approximately 1000  $\mu\text{m}$ , respectively. This is consequently reflected in the yearly pipe rupture probability results obtained from the Markov application analyses, as with the former distributions it is for most of the duration of the assumed operational plant lifetime approximately 100 times smaller than with the latter ones. This is a quite large difference, and indicates that the selection of the probabilistic distributions for initial sizes of SCC induced cracks during operation has a great impact on the consequent yearly pipe rupture probability results, an aspect which is useful to keep in mind e.g. when attempting to avoid unnecessary conservatism in the PFM and RI-ISI analyses. Concerning all cases and both input data sets, the yearly pipe rupture probability results vary approximately between 10E-10 to 10E-4. The assessment of the sizes of cracks initiating during plant operation as well as PFM analyses in general contain several sources of uncertainty, which subject is discussed in more detail in Chapter 4.

The accuracy of the rupture probability results summarised here is considered to be at least reasonable. However, more important than the absolute result values are their comparison to each other, since based on that the failure potential classes in the RI-ISI risk matrix failure potential category can be defined.

The average yearly rupture probability and cumulative rupture probability at 60 years for the 5 analysed piping welds for no inspections, and inspections at 10 and 5 year intervals are presented in Table 3.5.2-6 below.

*Table 3.5.2-6. The average yearly rupture probability and cumulative rupture probability at 60 years for the 5 analysed piping welds for no inspections, and inspections at 10 and 5 year intervals.*

Piping weld	Inspection interval [year]	Average yearly rupture probability [-]	Cumulative rupture probability at 60 y [-]
4-1-0--3	No inspections	0	0
	5	0	0
	10	0	0
4-1-0--4	No inspections	7.08E-07	4.18E-05
	5	8.33E-08	4.92E-06
	10	2.01E-07	1.19E-05
4-1-0--6	No inspections	2.01E-07	1.19E-05
	5	1.50E-08	8.88E-07
	10	4.26E-08	2.51E-06
4-1-3--8	No inspections	6.65E-07	3.92E-05
	5	8.53E-08	5.03E-06
	10	1.96E-07	1.16E-05
4-8-0--13	No inspections	2.48E-07	1.46E-05
	5	2.00E-08	1.18E-06
	10	5.58E-08	3.29E-06

## 4 Pipe leak/rupture probability analyses of the OL1 piping system 412

### 4.1 Short overview of the piping system

The piping system considered here is the Reheater and moisture separator system 412 located in the NPP unit OL1 of TVO. Similar Reheater and moisture separator system 412 is also located in NPP unit OL2 of TVO.

The main process functions of this piping system are to some extent reheat the cooled down water after it has gone through turbine, and before it is led back to the RPV via the Feed water system 312, and also to separate at certain areas moisture from the involved steam. The piping components of the system 412 are both of austenitic stainless steel and ferritic steel. The examined component, being of ferritic steel, is located on the condensate side of the system 412. It was assumed that the system 412 is among those few in BWR plants where FAC could potentially occur at some locations.

### 4.2 Input data for FAC analyses

The input data needed in the FAC analyses concerning the probabilistic wall thinning rate of the examined component of ferritic steel in the system 412 are briefly presented in the following. The analysis procedure was presented earlier in Section 2.2.2. The presented input data values here are approximate; however accurate values were used in the analyses. Also, the values of some parameters were to some extent varied in the FAC analyses. These are oxygen content and flow velocity, to both of which two values were given, which were kept analysis specifically as constant. The needed analysis input data were obtained from e.g. design drawings and material specifications provided by the TVO personnel experts, which are gratefully acknowledged. The approximate values of the input data needed in the FAC analyses concerning the probabilistic wall thinning rate of the examined ferritic component of the system 412 are presented in Table 4.2-1.

*Table 4.2-1. The approximate values of the FAC analysis input data; probabilistic wall thinning rate of the examined ferritic component of system 412.*

Fluid temperature	$T$ [K]	440
Geometry factor for straight tube	$k_c$ [-]	0.04
Nominal pipe wall thickness	$W_{original}$ [cm]	0.9
Pipe outer diameter	$D_{outer}$ [mm]	405
pH value	pH [-]	7
Oxygen content 1	$g1$ [ $\mu\text{g}/\text{kg}$ ]	0
Oxygen content 2	$g2$ [ $\mu\text{g}/\text{kg}$ ]	10
Cr+Mo content	$h$ [total %]	~0
Steel density	$\rho_{st}$ [ $\mu\text{g}/\text{cm}^3$ ]	7.80E+06
Assumed yearly exposure time	$t_{exposure}$ [h]	8000
Water flow rate 1	$F1$ [kg/s]	65
Water flow rate 2	$F2$ [kg/s]	70

The next step in the FAC procedure was to calculate case specifically the values for the intermediate input data parameters  $B$ ,  $N$ ,  $f(t)$  and  $\Delta\phi_R$ , by using formulas (2.2.2-3) and (2.2.2-4) presented in Section 2.2.2.

### 4.3 Results from the probabilistic FAC analyses

The results from the probabilistic FAC analyses performed in this study to the examined ferritic piping component of the system 412 are presented here.

The probabilistic FAC rate is calculated here as the product of its deterministic reference model prediction and an adjustment factor  $E$  [ - ], the probabilistic distribution of which is log-normal, and which accounts for the inadequacy of the calculated value. The presented results are 5<sup>th</sup>, 50<sup>th</sup> and 95<sup>th</sup> probability percentiles for the pipe wall corroded away,  $W_c(t)$ , for the assumed 60 years of operational lifetime as well as for the predicted durations to wall break (i.e. wall thinning reaches outer pipe surface). Also to be noted are the values of oxygen content and flow velocity which were to some extent varied in the analyses. The probabilistic FAC results are presented in Figures 4.3.1-1 to 4.3.1-4 and Table 4.3.1-1 in the following.

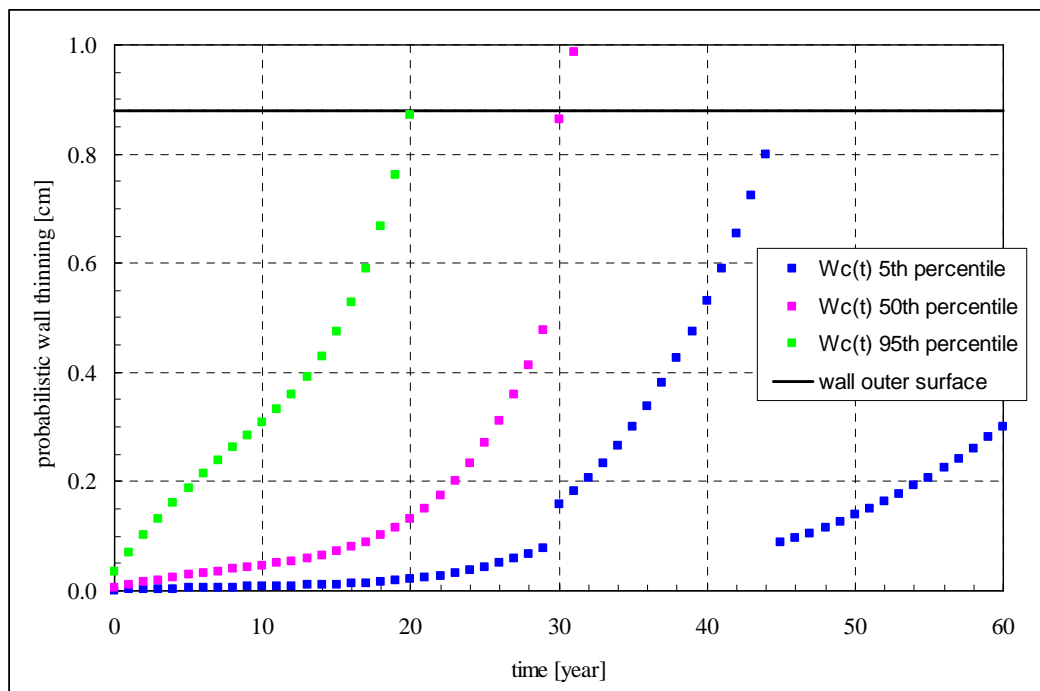


Figure 4.3.1-1. The 5<sup>th</sup>, 50<sup>th</sup> and 95<sup>th</sup> probability percentiles of the pipe wall corroded away for the examined ferritic component of system 412, when operational lifetime is assumed as 60 years. Here flow velocity is 63.3 kg/s and oxygen content is 0  $\mu\text{g}/\text{kg}$ .

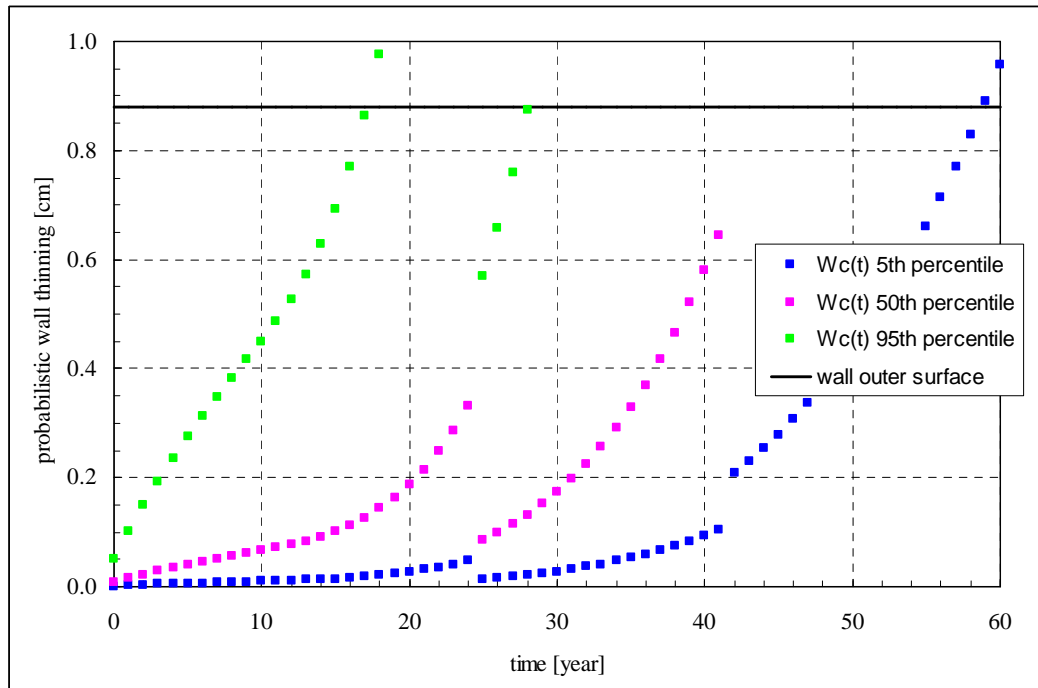


Figure 4.3.1-2. The 5<sup>th</sup>, 50<sup>th</sup> and 95<sup>th</sup> probability percentiles of the pipe wall corroded away for the examined ferritic component of system 412, when operational lifetime is assumed as 60 years. Here flow velocity is 63.3 kg/s and oxygen content is 10 µg/kg.

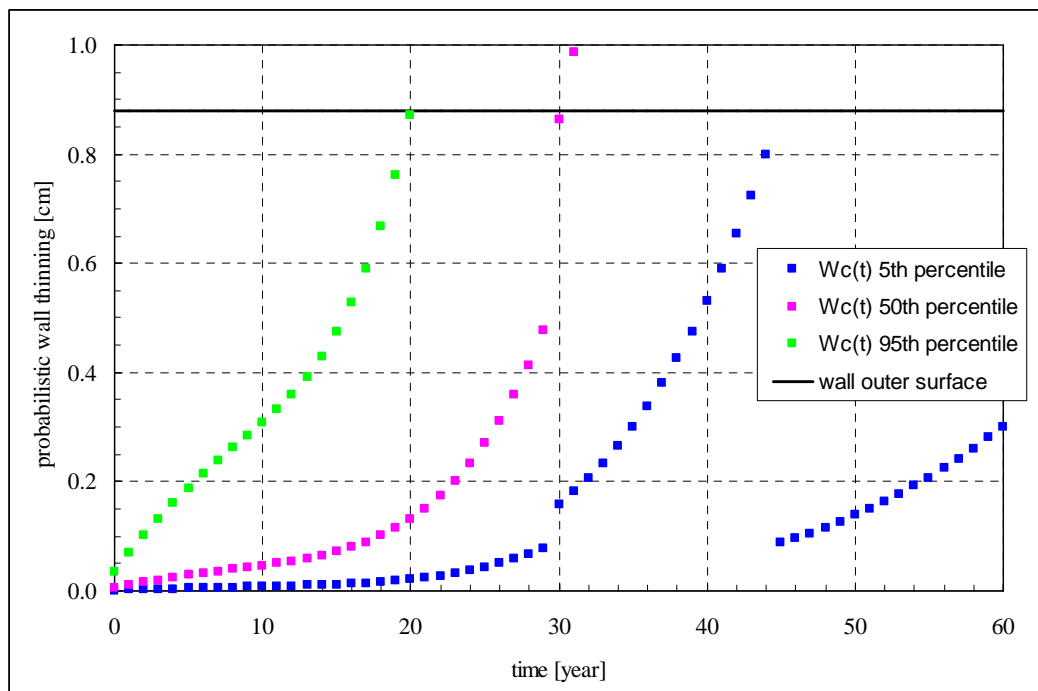


Figure 4.3.1-3. The 5<sup>th</sup>, 50<sup>th</sup> and 95<sup>th</sup> probability percentiles of the pipe wall corroded away for the examined ferritic component of system 412, when operational lifetime is assumed as 60 years. Here flow velocity is 71.5 kg/s and oxygen content is 0 µg/kg.

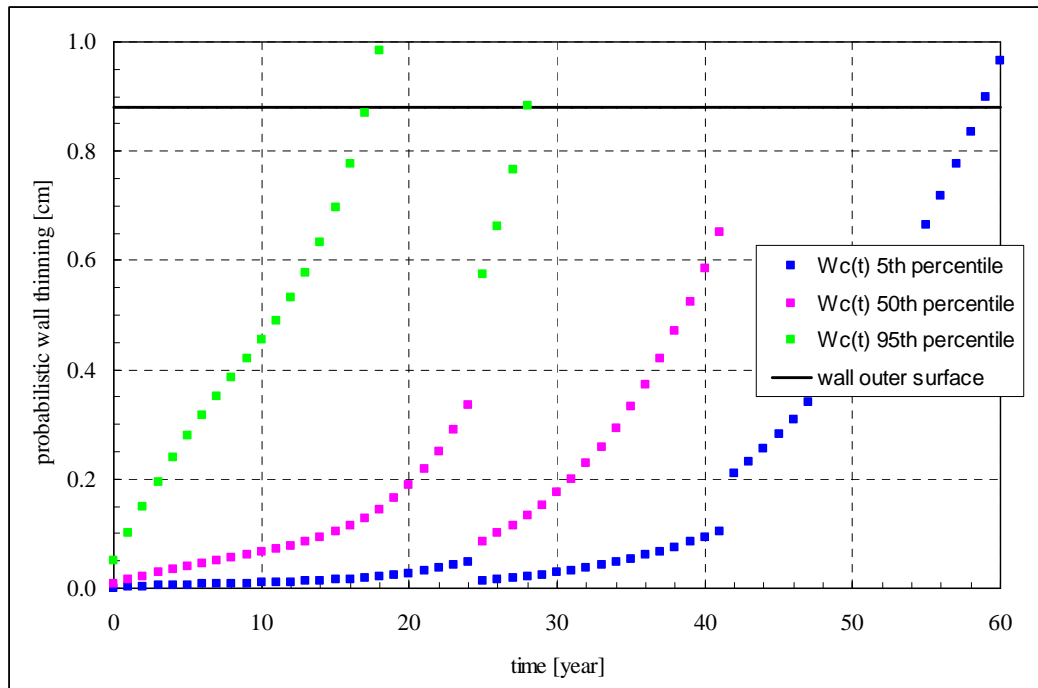


Figure 4.3.1-4. The 5<sup>th</sup>, 50<sup>th</sup> and 95<sup>th</sup> probability percentiles of the pipe wall corroded away for the examined ferritic component of system 412, when operational lifetime is assumed as 60 years. Here flow velocity is 71.5 kg/s and oxygen content is 10  $\mu\text{g}/\text{kg}$ .

The straightforward nature of the applied and to some extent conservative probabilistic FAC rate model, as taken from ref. [17], can also be noticed in the vertical offsets in some points of the presented result value distributions in Figures 4.3.1-1 to 4.3.1-4. Such behaviour of results is obviously not realistic. Here it is caused by the dependency of the adjustment factor on the calculated deterministic FAC rate. Namely, the dependency is divided to four categories, see Section 2.2.2, and the shift from one category to the next is slightly discontinuous. In one case, see 95th percentile distribution in Figure 4.3.1-2, result values reach the pipe wall outer surface even twice. In this case, as well as in other similar ones, the first i.e. earlier time the pipe wall outer surface is reached is to be taken as the correct result.

Table 4.3.1-1. The 5<sup>th</sup>, 50<sup>th</sup> and 95<sup>th</sup> percentiles for the predicted time durations to pipe wall break (i.e. wall thinning reaches outer pipe surface). Notations:  $F$  is flow rate,  $g$  is oxygen content.

Percentile	Predicted time duration to pipe wall break [year]			
	$F = 63.3 \text{ kg/s},$ $g = 0 \text{ } \mu\text{g}/\text{kg}$	$F = 63.3 \text{ kg/s},$ $g = 10 \text{ } \mu\text{g}/\text{kg}$	$F = 71.5 \text{ kg/s},$ $g = 0 \text{ } \mu\text{g}/\text{kg}$	$F = 71.5 \text{ kg/s},$ $g = 10 \text{ } \mu\text{g}/\text{kg}$
5 <sup>th</sup>	60	59	60	59
50 <sup>th</sup>	31	42	31	42
95 <sup>th</sup>	21	29	21	28



With this piping degradation analysis model it is quick and computationally very economical to obtain time dependent estimates of the probabilistic as well as deterministic wall thinning caused by FAC.

## 5 Summary and conclusions

Characteristics and development of RI-ISI methodology are examined in this report. This study continues earlier research work performed by almost the same project group, for a summary of which work see e.g. [10]. In this study the main emphasis was on developing the quantitative piping failure potential analysis capabilities, as well as widening their scope. This is realised using PFM based analysis procedures. In addition to a summary of this study, this chapter also includes conclusions as well as suggestions for further research.

### Summary and conclusions

Only the new RI-ISI related PFM analysis procedure developments and/or features are considered here. These include:

- assessment of probabilistic distributions for depth and length of SCC induced initial cracks,
- probabilistic assessment procedure for wall thinning of piping components due to FAC.

The developed approach to assess the probabilistic distributions of the sizes of initial cracks induced by SCC from the data of detected cracks is summarized here. So, the recursive assessment approach applied here is such that first the size data concerning detected grown SCC induced cracks, as obtained through screening from the used crack database, is converted to dimensionless form in relation to pipe wall thickness and inner circumference. Then, with fracture mechanics based analyses, the thus obtained data is matched with the assumed initial sizes, the criterion for which here is to correspond to respective mode I stress intensity factor threshold values,  $K_{I,threshold}$ , for SCC initiated cracks. Finally, the thus obtained data is converted to probabilistic form and a suitable reliability distribution function is fitted to it. The developed approach contains also uncertainties:

- Concerning the estimation of initial crack dimensions in general there are several uncertainties. As the data in the piping degradation databases concerns only detected grown cracks, the initial crack dimensions have to be assessed recursively, which is in several ways an uncertain process. Also, the applicable degradation data is often scarce and of questionable quality, which causes uncertainty as well.
- The crack growth equation used here, which has been correlated to crack growth propagation rate data from a considerable number of laboratory results, reflects the partly unknown differences between laboratory conditions and actual conditions in the plants.
- The definition of SCC nucleation threshold value for  $K_I$  is to some extent an ambiguous process as well.

In the light of the analysis results of this study it appears that when screening data from applicable crack databases to recursive assessments of probabilistic sizes of initial cracks induced by SCC, the effect of pipe size to the crack initiation has considerably less importance than pipe material. This would be because the probabilistic initial sizes obtained here are quite small, e.g. the mean value of the

probabilistic initial depth being of the scale of 300  $\mu\text{m}$ , which suggests that material property and environment chemistry associated characteristics hold much more responsibility for SCC induced nucleation of cracks than pipe size and stress distribution related ones (as regardless of the pipe size in the inner surface where these cracks nucleate tensile stresses typically prevail, especially in the piping welds).

The KWU-KR model [17], which is based on fitting of both detected and experimental data, has been selected for FAC analyses, because of the relevant FAC analysis models it is well documented in the published literature. The KWU-KR model [17] allows to some extent conservatively calculate the corrosion rate as a function of pipe geometry, material chemical composition, flow velocity, fluid temperature and fluid chemistry. With this model, the pipe wall thickness can be calculated as a function of time. To express uncertainty in the KWU model predictions, a probabilistic adjustment factor with a log-normal distribution is introduced to the deterministic reference model. The main result parameters from these FAC analyses include the time dependent 5<sup>th</sup>, 50<sup>th</sup> and 95<sup>th</sup> probability percentiles for the pipe wall corroded away as well as the predicted durations to wall break (i.e. wall thinning reaching outer pipe surface).

It is considered that improved PFM based analysis scope and accuracy provide valuable support to overall quantitative assessment of piping weld failure potentials. In general, the favoured option for quantitative piping failure potential assessment would be statistical analysis of piping degradation data. However, there most often does not exist enough applicable degradation data for this, and thus structural reliability methods, most relevant for this purpose being PFM, need to be resorted to. So, having both cracking data and PFM analysis results gives a much better and in scope wider information basis for experts to plant specifically assess the piping weld failure potentials, and consequently leads to more accurate and detailed RI-ISI analysis results. As with other RI-ISI related analysis procedures, also PFM has its uncertainties and accuracy challenges; however PFM analyses on the other hand easily allow making extensive sensitivity analyses for the involved physical analysis input parameters. It should be mentioned, though, that PFM analyses alone do not yet suffice to be the sole basis for piping failure potential quantification.

The accuracy of the analysis procedures summarised here is considered to be at least reasonable, and mostly or arguably in all cases to some extent conservative. Thus the results obtained with these PFM procedures are considered to be useful for quantitative RI-ISI analysis purposes, also due to providing the above mentioned new developments. However, more important than the absolute result values are their comparison to each other, since based on that the failure potential classes in the RI-ISI risk matrix failure potential category can be defined.

### **Suggestions for future research**

The estimates of initial crack sizes, both concerning manufacturing cracks and cracks initiating during operation, are a major source of uncertainty in PFM analyses, e.g. since relatively small changes in them have a quite strong impact on PFM analysis model response. Also, not many models for initial crack sizes exist, and mostly they appear quite crude. Thus, from the viewpoint of PFM and RI-ISI

analysis results quality, it would be advantageous to develop and refine these estimates more. Also from the research point of view this issue is highly interesting, as it involves several physical phenomena, and consequently scientific challenges including e.g. statistical mathematics and structural analyses. International crack databases could also provide useful data for estimating initial crack sizes. In this respect, especially access to the OPDE (OECD Piping Failure Data Exchange) database by OECD would potentially be advantageous, as it is an advanced good quality piping failure database containing cracking data from most countries having NPPs, see refs. [45, 46] and an analysis example in ref. [47].

Also, it would be useful to quantify and minimise the uncertainties in the developed approach to assess the probabilistic distributions of the sizes of initial cracks induced by SCC from the data of detected cracks, thus refining it by making it more accurate. This is because it was beyond the scope of this study to attempt to create such probabilistic distribution estimates that could be recommended to be used for practical applications in larger scale. Instead the purpose here was more to demonstrate the applied approach and point out the sources of uncertainty/inaccuracy. It is deemed here that with a wider scale of better quality database crack data and with more effort concerning minimising the mentioned uncertainties, more accurate probabilistic initial sizes for SCC induced initial cracks could be obtained, which would also better suit for practical PFM/RI-ISI analysis purposes. Another improvement could be to change the used reliability distribution from the exponential function with the cut-off to zero for a narrow region in the beginning, i.e. for the smallest crack sizes, to a log-normal one, so that the whole distribution could be covered with one reliability function without the need to use piecewise distribution approach.

The joint effect of degradation mechanisms would be a useful issue to cover as well. This is because the summed up effect of e.g. fatigue induced cracking and SCC, which joint phenomenon has been encountered in the existing cracking data, potentially leads to faster crack growth than when only one degradation mechanism per weld at a time is considered. Moreover, the resulting rate of degradation can be faster than the arithmetic sum of the considered degradation mechanisms. A starting point for considering the joint effect of degradation mechanisms, however, could be developing the PFM application to cover the aforementioned arithmetic sum of SCC with low-cycle and high-cycle fatigue.

Also fatigue due to unexpected transient load cases caused by thermal stratification of the water in the pipes could be added to the PFM analysis scope in the future. This form of fatigue degradation has been encountered e.g. in the surge line and in the feed water lines of the reactor coolant system [38], and has also been identified as a valuable research target by some representatives of Finnish energy companies.

It would also be advantageous to compare the piping leak/rupture probabilities calculated with VTTBESIT to those calculated with other PFM based cracking analysis codes, e.g. PIFRAP and ProSACC. A small PFM analysis tool benchmarking study will be carried out during 2008 and 2009 in the framework of the Nordic Nuclear Safety Research (NKS).

It is also the purpose to continue developing the LHS procedure that was added to VTTBESIT earlier in this project. One option that looks advantageous from the

viewpoint of cracking probability analyses is to combine LHS with stratified sampling. The basic idea of this combined sampling is as follows: according to the stratified sampling, the sample space of a dominant random variable (e.g., initial surface crack depth  $a_0$  or fracture toughness  $K_{Ic}$ ) is partitioned into  $m$  mutually exclusive sub-regions and the number of simulations in each sub-region is proportional to its contribution to the total fracture probability. Then, the estimated leak/break probability value of each crack size sub-region (i.e., each strata of the initial surface crack depth) is calculated with LHS.

The computational efficiency of analysis code VTTBESIT concerning SCC analyses could also be improved by optimising the time step selected for use in the analyses. This could be realised by lengthening it and checking then the model response, and based on that decide what would be the accurate enough optimised length for the time step.

The Markov process analyses could be developed e.g. by refining the formulation of both degradation and inspection matrices. As for the former matrix, in the present application an yearly mean value is assessed over the whole of the assumed operational plant lifetime. This means that for each year the degrading conditions/potential is consequently assumed to be the same. However, when considering originally dormant and later on more aggressively progressing degradation mechanisms, such as SCC, it appears to be more realistic to divide the operational lifetime to two or more parts, according to different experienced phases in severity of degradation, which in turn could be assessed based on world-wide as well as plant specific databases. On the procedure side this would require developing a piecewise continuous version of the Markov process application. In which the Markov properties would e.g. be required only within the time step in question, the duration scale of which could be a decade or two, and then setting the ending conditions of this analysis time step as starting conditions to the next one. The technical soundness of this development approach, or any other for this purpose, remains yet to be confirmed, however. As for the inspection matrix, the present Markov analyses were limited to produce the failure probability estimates from the VTTBESIT simulations with rather simple considerations of inspection strategies. More investigations of the effect of various inspection reliability and interval assumptions on the failure probability estimates should be carried out.

## References

1. Gosselin, S. R. EPRI's new in-service pipe inspection program. Nuclear News, November 1997. pp 42-46 .ISSN 0029-5574.
2. Tupala, M. Ydinvoimalaitoksen riskitietoinen putkitarkastuksen optimointi. Master's thesis. Tampere University of Technology. 54 p. 2002. (In Finnish)
3. Gosselin, S. (Project Manager). Risk-informed inservice inspection evaluation procedure. Electric Power Research Institute, Interim Report EPRI TR-106706. California, 1996.
4. Simola, K., Holmberg, J., Cronvall, O., Männistö, I., Vepsä, A. RI-ISI pilot study of the Shut-down cooling system of the Olkiluoto 1/2 NPP units. VTT Industrial Systems, Espoo. Research report: TUO72-051318. 2005. 44+23 p.
5. Fleming, K., N., Gosselin, S. Application of Markovian Technique to Modeling Influences of Inspection on Pipe Rupture Frequencies", Proceedings of the seminar on piping reliability, Swedish Nuclear Power Inspectorate, Sigtuna Sweden, September 30-October 1, 1997.
6. Fleming, K., N. Markov models for evaluating risk-informed in-service inspection strategies for nuclear power plant piping systems, Reliability Engineering & System Safety, Elsevier Science 2004, 19 pages.
7. Cronvall, O., Holmberg, J., Männistö, I., Pulkkinen, U. Continuation of the RI-ISI pilot study of the Shut-down cooling system of the Olkiluoto 1/2 NPP units. VTT Industrial Systems, Espoo. Research report TUO72-056667, 2006. 60 p.
8. Besuner, P., M., Probabilistic fracture mechanics. In: Provan, J.W. (ed.). Probabilistic Fracture Mechanics and Reliability. 1987, Martinus Hijhoff Publishers. pp. 325 - 350.
9. Brückner, A., Numerical methods in probabilistic fracture mechanics. In: Provan, J.W. (ed.). Probabilistic Fracture Mechanics and Reliability. 1987, Martinus Hijhoff Publishers. pp. 351-386.
10. Cronvall, O., Männistö, I., Simola, K. Development and testing of VTT approach to risk-informed in-service inspection methodology - Final report of SAFIR INTELI INPUT Project RI-ISI. VTT Research Notes 2382, Technical Research Centre of Finland (VTT). April 2007, Espoo. 43 p. Online version available at: <http://www.vtt.fi/publications/index.jsp?lang=en>
11. Cronvall, O., Simola, K., Vepsä, A., Alhainen, J. RI-ISI pilot study of the Auxiliary feed water system of the Olkiluoto OL1 NPP unit. VTT, Espoo. Research report No. VTT-R-01414-08, 2008. 61 p.
12. Bergstrand, N. TVO I/II Modernization, System 311, 313, 314, 321, 321, 323, 326, 327, 351, 354 – Class 1, Summary of Temperature Loads. ABB Atom AB, Report PAB 96-258. 24.10.1996. 41 p.
13. SINTAP; Structural Integrity Assessment Procedures for European Industry; Final Procedure: November 1999. Project funded by the European Union (EU) under the Brite-Euram Programme: Project No. BE95-1426, Contract No. BRPR-CT95-0024.

14. Hazelton, W.S., Koo, W.H. Technical Report on Material Selection and Processing Guidelines for BWR Coolant Pressure Boundary Piping. Springfield. U.S. Nuclear Regulatory Commission (NRC), Office of Nuclear Reactor Regulation, NUREG-0313-Rev2-F, Final Report. U.S., Jan 1988. 25 p.
15. Wellein, R., Applications of FM in the nuclear industry to reactor pressure vessel, main coolant piping and steel containment. In: Provan, J.W. (ed.). Probabilistic Fracture Mechanics and Reliability. 1987, Martinus Hijhoff Publishers. pp. 387-436.
16. Smith, C., L., Shah, V., N., Kao, T., Apostolakis, G. NUREG/CR-5632, Incorporating Aging effects into Probabilistic Risk Assessment — A Feasibility Study Utilizing Reliability Physics Models. U.S. Nuclear Regulatory Commission, 2001. 131+112 p.
17. Kastner, W., Riedle, E. Empirical model for calculation of material losses due to corrosion erosion. VGB Kraftwerkstechnik 66 12 (1986), pp. 1023–1029.
18. Chopra, O., K., Shack, W., J. Environmental Effects on Fatigue Crack Initiation in Piping and Pressure Vessel Steels. NUREG/CR-6717, Technical Report. U.S. Nuclear Regulatory Commission (NRC), May 2001. 86 p.
19. Kastner, W., 1987. Erosion-Corrosion Experiments and Calculation Model, EPRI Workshop on Erosion-Corrosion of Carbon Steel Piping: Nuclear and Fossil Plants, April 14-15.
20. Mononen, J. et al. Pilot-tutkimus tarkastustoiminnan (in-service inspection) kohteiden riskiavusteisesta priorisoinnista. Final report. The Finnish Radiation and Nuclear Safety Authority (STUK), 2000. (in Finnish)
21. Brickstad, B., Josefson, B., L. A parametric study of residual stresses in multi-pass butt-welded stainless steel pipes. International Journal of Pressure Vessel and Piping, Vol. 75, 1998. Pp. 11-25.
22. Chapman, V., 1993. Reliability and risk in pressure vessels and piping, Proceedings of the Simulation of Defects in Weld Construction, Pressure Vessel and Piping Conference, American Society of Mechanical Engineers, New York, PVP-251, pp. 81 - 89.
23. Provan, J., W., Probabilistic approaches to the material-related reliability of fracture-sensitive structures. In: Provan, J.W. (ed.). Probabilistic Fracture Mechanics and Reliability. 1987, Martinus Hijhoff Publishers. pp. 325 - 350.
24. Simonen, F.A., Khaleel, M. A. Uncertainty analyses of probabilistic fracture mechanics calculations of piping failure probabilities. Proceedings of the 4th International Conference on Probabilistic Safety Assessment and Management, 13–18 September 1998, New York, Probabilistic Safety Assessments and Management PSAM 4, Vol. 3, pp. 2040 - 2045.
25. Anderson, T., L. Fracture Mechanics, Fundamentals and Applications. Third edition, CRC Press, 2004. 730 p.



26. Bergstrand, N. TVO I/II Modernization - System 311, 313, 314, 321, 323, 326, 327, 351, 354 – Class 1 Temperature Loads. Report PAB 96-116, ABB Atom AB, Rev. 1.7.10.1996. 56 p.
27. ASME Boiler and Pressure Vessel Code, Section II. 2004.
28. ABB ATOM Materialhandboken - Normer och datablad för metalliska material. ABB Atom AB, 1999.
29. Bergman, M., Brickstad, B., Dahlberg, L., Nilsson, F. and Sattari-Far, I. A procedure for safety assessment of components with cracks - Handbook. SAQ/FoU-Report 96/08, SAQ Kontroll AB, 1996. 104 p.
30. ASME Boiler and Pressure Vessel Code, Section XI. Edition 2004.
31. 323-yhteen safe endin ja putkiston välisen hitsin kohdalle oletettujen säröjen tarkastelu. Technical Research Centre of Finland (VTT), Manufacturing Technology, Research Report VAL64-7024/97.
32. Fracture mechanics investigation of the safe-end of core spray system 323. Siemens Aktiengesellschaft, KWU, Work-Report U9 213/88/e53+U9 213/Ba/Kb 05.05.1988. 33 p.
33. Jansson, C., Morin, U. Assessment of Crack Growth Rates in Austenitic Stainless Steels in Operating BWRs. Proc. of Eighth International Symposium on Environmental Degradation of Materials in Nuclear Power Systems - Water Reactors. August 10 - 14, 1997. Amelia Island, Florida. Pp. 667 - 674.
34. Roark, R., Young, W. Formulas for Stress and Strain. Fifth Edition. McGraw-Hill Book Company, U.S.A., 1975. 624.
35. Brickstad, B. The Use of Risk Based Methods for Establishing ISI-Priorities for Piping Components at Oskarshamn 1 Nuclear Power Station. SAQ/FoU-Report 99/05, SAQ Kontroll AB, 1999. 83 p.
36. Olkiluoto Nuclear power plant units 1 and 2. Teollisuuden Voima Oy (TVO), 1998. 42 p.
37. Paris, P., C., Erdogan, F. A Critical Analysis of Crack Propagation Laws. Journal of Basic Engineering, Vol. 85, 1960, pp. 528 - 534.
38. European Commission. Nuclear Safety and Environment. Safe Management of NPP Ageing in the European Union, Final Report, 2001. 363 p.
39. Jones, H., R. (Editor). Stress-Corrosion Cracking. ASM International, Ohio, 1992. 448 p.
40. Congleton, J., Craig, I., H. "Corrosion Fatigue" in Corrosion Processes, Parkins, R., N., Ed., Applied Science Publishers, 1982.
41. Varfolomeyev, I. et al. BESIF 1.0: Stress Intensity Factors for Surface Cracks under 2D Stress Gradients. IWM-Report T 14/96, Fraunhofer-Institut für Werkstoffmechanik (IWM), July 1996. 42 p.
42. Busch, M. et al. KI-Factors and Polynomial Influence Functions for Axial and Circumferential Surface Cracks in Cylinders. IWM-Report T 18/94, Fraunhofer-Institut für Werkstoffmechanik (IWM), October 1994. 41 p.

43. Busch, M. et al. Polynomial Influence Functions for Surface Cracks in Pressure Vessel Components. IWM-Report Z 11/95, Fraunhofer-Institut für Werkstoffmechanik (IWM), January 1995. 88 p.
44. Vepsä, A. Verification of the stress intensity factors calculated with the VTTBESIT software. Technical Research Centre of Finland (VTT), Research Group Structural Integrity, Research Report TUO72044578. 40+2 p.
45. OECD. 2005. OECD-NEA Piping Failure Data Exchange Project (OPDE), Workshop on Database Applications. OPDE/SEC(2004)4. Nuclear Energy Agency, Issy-les-Moulineaux, France.
46. OECD. 2006. OPDE 2006:1 Coding Guideline (OPDE-CG) & OPDE User Instruction. PR01 Version 02, Restricted Distribution. Nuclear Energy Agency, Issy-les-Moulineaux, France.
47. Simonen, F., A., Doctor, S. R. et al. Probabilistic Fracture Mechanics Evaluation of Selected Passive Components - Technical Letter Report. Pacific Northwest National Laboratory (PMML), U.S.A., May 2007. 96 p.